

N72-2323

Final Report

A SEISMIC SURVEY OF THE MANSON DISTURBED AREA

**CASE FILE  
COPY**

Lyle V.A. Sendlein  
Professor of Geophysics  
Department of Earth Science  
Iowa State University  
Ames, Iowa

Thomas A. Smith  
Geophysicist  
Chevron Oil Company  
Houston, Texas

National Aeronautics and Space Administration  
Grant NGR 16-002-028

October 25, 1971

Science and Humanities Research Institute  
Iowa State University  
Ames, Iowa

## ABSTRACT

The region in north-central Iowa referred to as the Manson disturbed area was investigated with the seismic refraction method and the bedrock configuration mapped. The area is approximately 30 km in diameter and is not detectable from the surface topography; however, water wells that penetrate the bedrock indicate that the bedrock is composed of disturbed Cretaceous sediments with a central region approximately 6 km in diameter composed of Precambrian crystalline rock.

Seismic velocity differences between the overlying glacial till and the Cretaceous sediments were so small that a statistical program was developed to analyze the data. The program developed utilizes existing 2 segment regression analyses and extends the method to fit 3 or more regression lines to seismic data.

The seismic data was collected on two-mile centers as reversed profiles. The data was analyzed and depths and velocities were determined and plotted as two separate maps. The resulting bedrock topography includes closed depressions, but the circular pattern observed in the subsurface data is not reflected in the bedrock topography. Bedrock seismic velocity patterns appear to correlate with the Bouguer gravity map developed in an earlier study. The Precambrian crystalline rock displayed velocities ranging between 3000 m/sec to 5000 m/sec whereas the disturbed sediments ranged between 2000 m/sec to 3000 m/sec.

The study was not able to provide the necessary data to establish the origin of the crater. The bedrock configuration map and the velocity distribution map do point to another crystalline subcrop west and south of the present outcrop.

## TABLE OF CONTENTS

	Page
INTRODUCTION	1
COLLECTION OF THE SEISMIC DATA	9
STATISTICAL METHOD	12
Background	12
Unconstrained Join Type	15
Constrained Join Type	19
An Algorithm	23
Examples	26
ANALYSIS OF NEAR-SURFACE VELOCITIES	32
Selection of Data	32
Statistical Analysis	33
ANALYSIS OF DEEPER VELOCITIES	37
Statistical Analysis	37
Velocity Distributions	38
VELOCITY CONSIDERATIONS	42
Dipping Refractors	42
Velocity Anisotropy	50
Velocity Reversals and Hidden Layers	50
Velocity Contrast	52
BEDROCK VELOCITY AND TOPOGRAPHY	54
DISCUSSION	59
LITERATURE CITED	62
ACKNOWLEDGEMENTS	65
APPENDIX A. LIST OF THE COMPUTER PROGRAM	66
APPENDIX B. TABULATION OF PREFERRED REGRESSION FITS	94

## LIST OF TABLES

	Page
Table 1. Statistical fits of first 100 maximum times	35
Table 2. Opposite-intercept test of 23 sites that had passed 2-layer slope test for a 2-layer dipping layer model	49
Table 3. Test data of distance, d, and time, t	68
Table 4. Comparison of three computer programs	68
Table 5. Significant figures of the calculation of residual sum of squares for various values of time	69
Table 6. Tabulation of preferred regression fits	95

## LIST OF FIGURES

	Page
Figure 1. General geologic map of the Manson disturbed area with seismic refraction and borehole locations	3
Figure 2. Aeromagnetic map of the Manson disturbed area	6
Figure 3. Bouguer gravity anomaly map of the Manson disturbed area	7
Figure 4. Two segment regression fit of typical shallow refraction data	27
Figure 5. Three segment regression fit of typical shallow refraction data	29
Figure 6. Scatter diagram of all time-distance measurements	34
Figure 7. Distribution of seismic velocities by layer	39
Figure 8. Slope test of all seismic sites by line segment	48
Figure 9. Bedrock velocity graph and contour map of the Manson disturbed area	53
Figure 10. Bedrock topographic contour map of the Manson disturbed area	57

## INTRODUCTION

The identification of granitic well cuttings by the Iowa Geological Survey from water well samples taken near the town of Manson, Iowa, suggested that an unusual geologic feature was buried at relatively shallow depths beneath glacial drift that blankets most of Iowa. A number of water wells drilled into bedrock near the wells from which the granitic cuttings were taken, revealed that the normal sequence of bedrock formations did not exist in the region. Moreover, the cuttings from these wells were highly deformed. The Iowa Geological Survey established a boundary enclosing all of these wells and labeled the region the Manson disturbed area.

In an endeavor to explain the occurrence of the granitic rock and anomalously soft well-water in this region, the Iowa Geological Survey and U.S. Geological Survey conducted a drilling program near Manson in 1952. From a bore hole, drilled approximately 6 km north of Manson, 118 m of crystalline core was recovered below 28 m (93 ft.) of glacial drift.

Petrologic analysis showed that it consisted of highly deformed gneiss, gneissoid granite, granite, and diabase, all Precambrian in age (Hoppin and Dryden, 1958). The dimensions of the major components of each rock type were also varied. Breccias, with rock fragments as long as 45 cm grading down to chloritized microbreccia, made up a large part of the core. Weathering alterations occurred as deep as 60 m into the crystalline material (Dryden, 1955). Lidiak et al. (1966) have dated the crystalline rock by the Rb-Sr method to be between  $1.13$  and  $1.44 \times 10^9$  years. Bunch (1968) found that the minerals in the crystalline mass had numerous unusual microstructures. Quartz had well-defined multiple kink bands, and deformation bands

in plagioclase were observed.

After an examination of available well logs, both Dryden (1955) and Hoppin and Dryden (1958) suggested that the crystalline rock surface is nearly flat-topped and covers an area approximately  $4 \text{ km}^2$  directly beneath the glacial drift. Extending beyond this area, the surface of the crystalline rock falls away in all directions with steeper slopes to the southeast. They concluded that the Manson disturbed area has many similarities with the characteristics of cryptovolcanic features as outlined by Bucher (1936). Bunch (1968) concluded that the numerous structural features in the minerals indicated that the Manson disturbed area had undergone violent disruption. Irrefutable evidence that the area had been subjected to shock pressures that only a meteorite could produce, such as shock-formed glass and/or high pressure silica polymorphs, had not been discovered in the thin sections.

A compilation of elevations of the basement rock of Iowa by Yoho (1967) shows that at two locations in Ft. Dodge the top of the basement rock is 315 and 399 m below mean sea level and is typical of north central Iowa. The elevation at which the crystalline rock was found north of Manson by Hoppin and Dryden (1958) was 351 m above mean sea level. Therefore, the relief of the crystalline rock in the Manson disturbed area must be near 700 m.

A ground water resource study of Webster County by Hale (1955) suggested that the regional structure in the Manson area was abruptly broken by faulting, forming a roughly circular basin. Figure 1 is a geologic map of the Manson area as presented by the Iowa Geological Survey (1969). The Precambrian subcrop is shown surrounded by highly deformed lower Cretaceous shales. Mississippian limestones and dolomites border the disturbed area on

Kcd						
Ku						
Jfd						
Pch						
Mm						
Mk						
pEc						

Colorado and Dakota Groups. Sandstone and shale with minor limestone.

Cretaceous Undifferentiated. Variably calcareous, severely deformed shales, minor sandstone and carbonate rock.

Ft. Dodge Beds. Gypsum and red and green shale.

Cherokee Group. Cyclic deposits with carbonaceous shale, clay, siltstone, sandstone, and thick coal beds; minor, but persistent limestone beds.

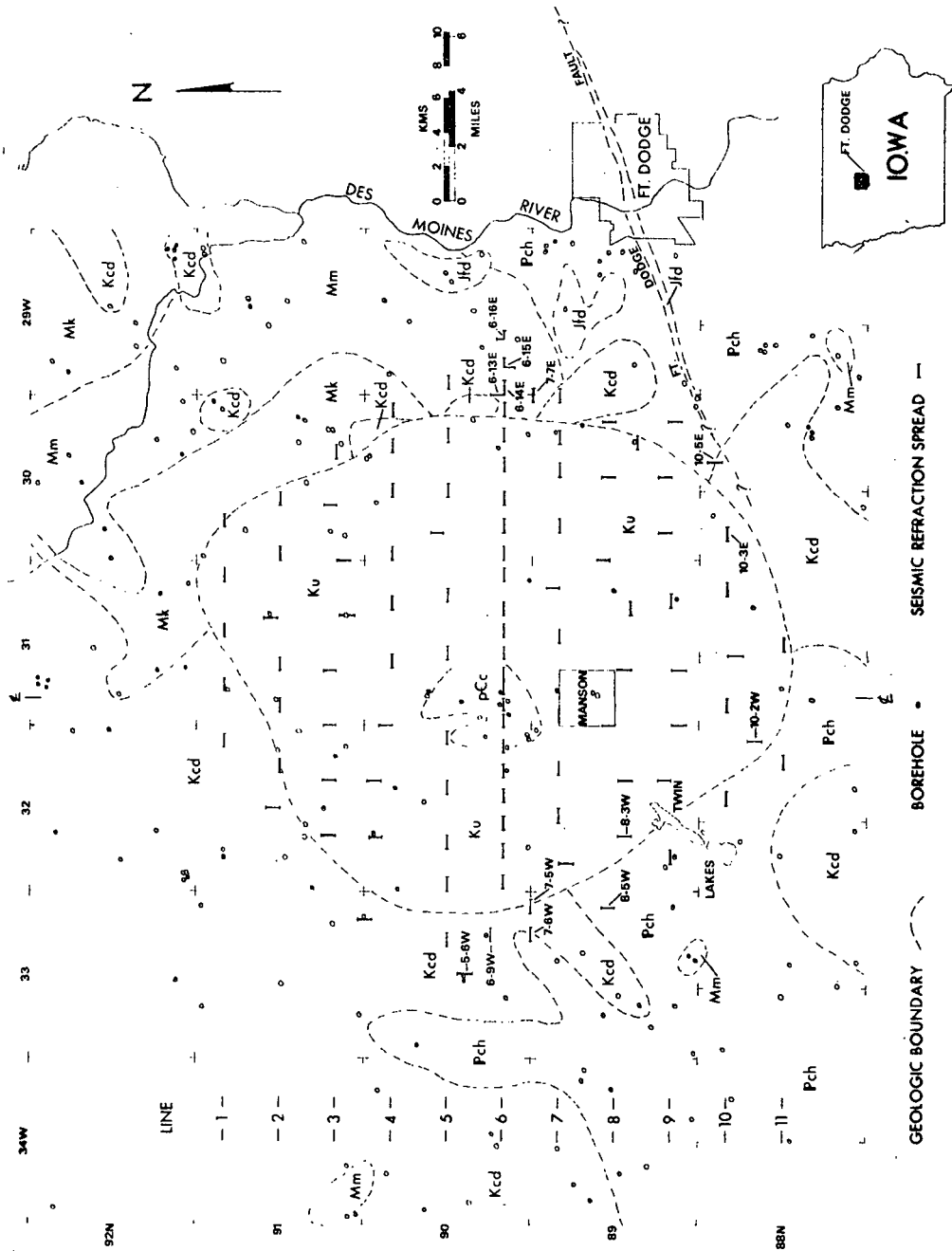
Meramec Series. Mainly St. Louis limestone: limestone and dolomite, sandstone locally predominant; locally contains chert.

Kinderhook Series. Mainly Gilmore City Limestone: light gray, fossiliferous limestone, commonly oolitic; Hampton Formation: limestone and dolomite; fossiliferous gray chert in lower portion; and Prospect Hill Formation: greenish-gray siltstone.

Crystalline Rocks. Includes granite, gneiss, and gneissoid granite; Rb-Sr dates 1.13-1.44 B.Y.

Figure 1. General geologic map of the Manson disturbed area with seismic refraction and borehole locations





the east, and Cretaceous shales and sandstones border on the north, west and south.

In 1953 an aeromagnetic survey was flown over the disturbed area (Henderson et al., 1963), and the resultant map was incorporated into a regional aeromagnetic map of central and southeast Iowa (Henderson and Vargo, 1965). Figure 2 is a reproduction of a portion of the 1953 survey. A magnetic high with a peak value of 4470 gammas roughly coincides with the outline of the crystalline rock as established from borehole information. Also prominent on the aeromagnetic map are several other anomalies. An elongate anomaly, trending NW-SE and having an intensity of 4605 gammas, is centered at a point 6 km northwest of Manson. Smaller anomalies (4115 and 3620 gammas) are located further from the center of the structure.

Holtzman (1970) recently completed a gravity survey of the disturbed region. He found that the regional effect of the mid-continent gravity high, which lies to the southeast of the Manson disturbed area, could be minimized with a trend surface technique that was successfully applied by Coons, Woollard and Hershey (1967) to similar gravity data. The Bouguer gravity map is shown on Figure 3. Holtzman found that a negative Bouguer anomaly in the interior of the disturbed area reflected, in part, low density brecciated sedimentary rock. Residual maps, calculated from as high as sixth degree trend surfaces, suggested to Holtzman that a peripheral graben bounds the eastern and southern edge of the Manson disturbed area, and that an inner arcuate fault paralleling the graben might also be located roughly equidistant between the center of the structure and the graben. Holtzman concluded that the gravity data from Manson had an appearance similar to gravity data from impact features. With this information at

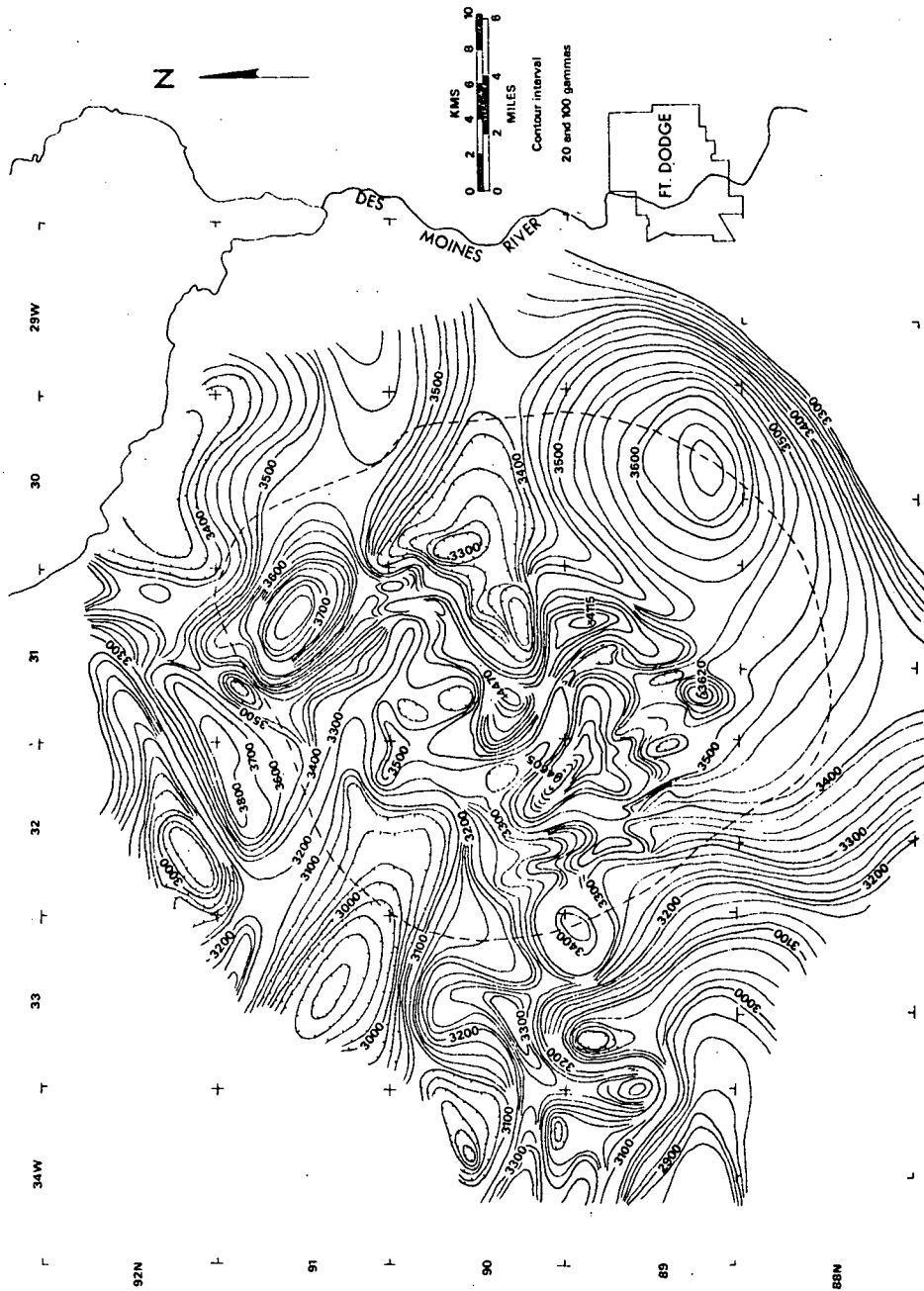


Figure 2. Aeromagnetic map of the Manson disturbed area

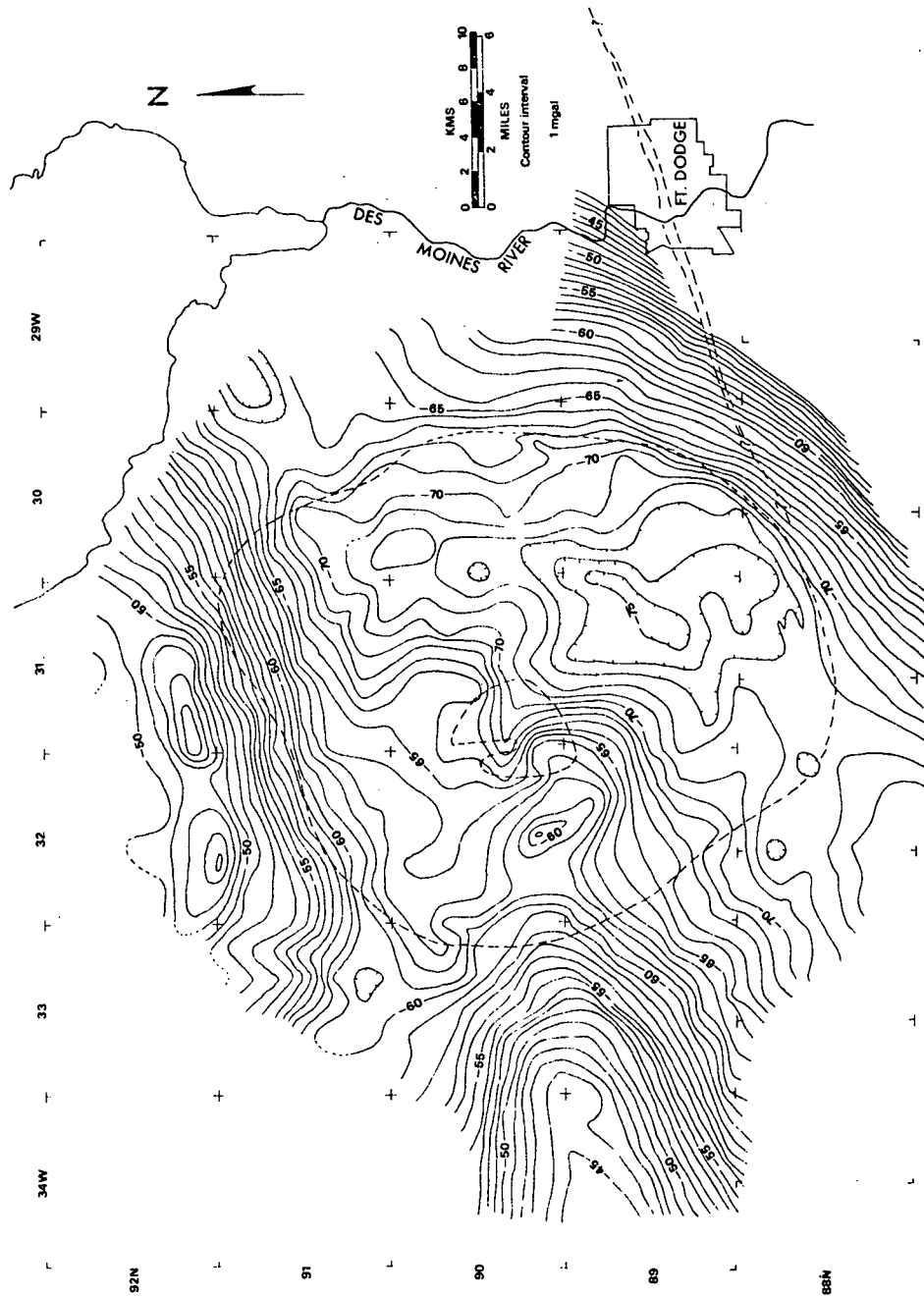


Figure 3. Bouguer gravity anomaly map of the Manson disturbed area

hand the seismic refraction study was initiated to investigate the nature and configuration of the upper portion of the Manson disturbed area.

## COLLECTION OF THE SEISMIC DATA

A total of 107 seismic locations were occupied in the course of the investigation. The data were collected at sites loosely fitting a 3.2 x 3.2 km (2 x 2 mi.) grid to take advantage of the spacing of the county roads in the area. In many cases the seismic locations could not be exactly located at the grid points because it was necessary to avoid primary roads, farm drainage tiles, and electric hi-lines. For identification purposes, the seismic sites were numbered along profile lines east or west of a north-south trending center line. The center line was drawn 1.6 km (1 mi.) east of the west edge of the townships in range 31W, and 11 profile lines perpendicular to the center line were drawn with a spacing every 3.2 km (2 mi.). See Figure 1. An example of the identification of a station would be the seismic site marked 3-2E. It would be the second seismic site east of the center line on line 3. Where a seismic site lies between two profile lines, the number is marked on the figure. All grid locations were occupied except 8-4W and 10-4E.

The seismic data were collected with a truck-mounted, 24-channel, analog, seismic recorder. Single 14 Hz geophones were spaced 32 m apart along two 12-channel seismic lines. The low-pass filters on the amplifier banks were locked out so that the lower effective frequency was the 14 Hz of the geophone response. A high-pass filter of 120 Hz was used throughout the field operation. Amplifier gains were adjusted to enhance the first arrival breaks. Timing on the seismic records was marked by timing lines spaced 0.010 seconds apart. Two independent 100 Hz oscillators were simultaneously recorded and later checked against each other, giving a precision of the

lines better than 0.001 second in five seconds.

Two basic geophone spread configurations were employed. At 29 locations, most of which were along line 6, a split spread geometry was used, and a charge was detonated between them. This geometry produced two sets of 12 arrival times for each shot. In several locations on the eastern side of the study area in the undisturbed region, the two cables were strung perpendicular to each other; in this fashion the presence of a marker horizon below the bedrock surface might be used to detect the true bedrock dip. Also at 13 other sites, a second charge was detonated at one end of the seismic line so that true reversed profiling might be accomplished on 12 traces. At the 78 other sites, the spread geometry consisted of stringing the cables along a straight line, and charges were detonated at each end of the seismic line. This geometry produced 24 arrival times for each shot.

Five to six pound (about 25 NT) charges of 40% strength stick dynamite were buried at a depth of approximately 3 m in the glacial drift. The charge was placed beyond the farthest geophone at a distance in line with the seismic line of from 20 to 60 m and at a distance perpendicular to the line of from 3 to 15 m.

From the seismic recordings the first arrival times and time breaks were picked with a 3X power binocular microscope mounted with an eyepiece reticule. Three trained observers analyzed several records, and a comparison showed that the arrival times could be picked with a precision of  $\pm 0.002$  seconds. Because the mechanical alignment of the galvanometer and timing line optics in the recording oscillograph cannot be accurately assured below this level, the overall accuracy of the arrival time determinations was sufficiently low to warrant the use of one observer for the

bulk of the data.

The raw time values and distances were encoded and digitized. Each coding form was sight verified with the original seismic record, and the digital records were then mechanically verified with the coding forms. Several consistency checks were made on the digitized data. As an example, on 24 trace records the time shift and offset distances on traces 1-12 were compared to those of traces 13-24, and the difference in ground distance between trace 12 and 13 was checked against the standard takeout spacing.

Several corrections were applied to the time and distance data. A relay closure time of 0.001 second was added to each of the raw first arrival times. The horizontal distance from shot point to geophone for each arrival time was corrected for the distance the shot point was offset from the seismic line. The relief along the geophone spread was usually less than 5 m; only in one instance was the relief as great as 15 m. Because of this low relief, time corrections due to topography were not calculated.

A reconnaissance altimeter survey of many of the gravity stations established by Holtzman (1970) confirmed his published  $\pm 1.2$  m elevation accuracy. For each seismic location an altimeter loop was tied from the seismic shot points to the nearest gravity station. The horizontal datum plane for each shot, from which the depth calculations were made, was set at an elevation,  $E$ , such that  $E = E_{\text{shot}} - C/2$ , where  $E_{\text{shot}}$  is the elevation of the top of the shot hole and  $C$  is the depth to the center of charge. Therefore the accuracy of the elevations of the refracting horizons is within  $\pm 2.5$  m.



## STATISTICAL METHOD

In the development of the refraction method, it was immediately realized that there was some reproduceable linear relationship between the source-to-receiver surface distance and the time of arrival of the seismic energy. The exact linear relationship, as inferred from geometrical optics, is often expressed as a line segment on a time-distance plot of the data, and the least squares method has been used to 'best fit' these line segments to the data.

### Background

The statistical implications of the 'best fit' regression analysis have not, until recently, been appreciated. Steinhart and Meyer (1961) have reviewed the use of statistical uncertainty in seismic refraction, and they have concluded that the results of seismic refraction investigations have seldom been presented with estimates of uncertainty.

Because the error of measurement of distance is normally several orders of magnitude less than the error of the measurement of time, as a reasonable approximation, the error associated with the data may be considered to arise only from time. The measurement of distance is then taken to be without error. From this, all deviation from the time value predicted by this linear relationship are thought to arise from the error of the measurement of time only.

The principle of least squares states that the best estimate of the true time value at a distance is one that minimizes the sum of the squares of the time deviations from their estimates. The wave slowness and time intercept, determined with least squares regression, are used as

coefficients of the regression line of best fit. But by the admission of error, there cannot be considered an 'exact' functional relationship between time and distance, and so, the measurement of the coefficients is also subject to error.

No assumption as to the distribution of time deviations at a distance need be made. The principle of least squares does not imply the normal distribution of errors, only that the estimated parameters are unbiased and have minimum variance. Borchardt and Healy (1968), in fact, suggest that for crustal refraction data, the distribution is not normal but is more peaked than normal. Regardless of whether or not it is, the central limit theory states that the distribution of the sum of a number of small errors will approach a normal distribution when the number of measurements grows large. If no assumption as to the distribution of time error at a particular distance is made, or no measure of the distribution is attempted, only the determination of the slope and time intercept parameters with the method of least squares may be made. Ultimately the time deviations at a distance are not as important as the ability of the model to fit the situation.

The method of least squares was first used to choose the line that 'best fit' the data over a range of distances chosen by the seismologist. Steinhart and Meyer (1961) presented the uncertainty of the wave slowness and time intercept for a line segment under the assumption that the error of time was normally distributed. Statistics may further be used to choose the 'best fit' combination of line segments for the entire range of distances over which the refraction data was collected. This problem has not been attacked in the field of seismology. The problem has only recently been investigated by those in the field of statistics.

Sprent (1961) considered the determination of the critical value of the independent variable when there were known to be two connected regression lines. Quandt (1958b) considered the estimation of parameters when the regression system obeys two separate regimes. He concluded that some previous determination must be made as to the number of regressions present in the system. Several difficulties were encountered by Quandt (1958a) when he attempted to establish statistical tests to determine this number. Robinson (1964) investigated the change-over value for polynomial regressions. Hudson (1966) presented the general solution to the estimation of parameters and change-over values for both linear and higher order polynomial regressions.

Two computational schemes, following Hudson's guidelines, have been developed to estimate the number of regressions which will fit a set of data. Bellman and Roth (1969) have used a dynamic programming approach, and McGee and Carleton (1970) have applied the method of cluster analysis.

Recently seismologists have approached the determination of join point (or critical distance) by using selective data rejection. Iyer et al. (1969) used an iterative scheme which rejects data with high time deviations. Segments of the data are selected to be fitted, and at each successive iteration, data points which deviate from the calculated regression line by some specified level are rejected from subsequent calculations. The curve fitting method formulated by Kaila and Narain (1970) differs from the method used by Iyer et al. in that weights are assigned to each data point. The weights are assigned on the basis of the normal probability function for the time error. Then the regression for each line segment is calculated using all the data points weighted for that particular regression. Because of slow

convergence, however, Kaila and Narain found it necessary to revert to data rejection in the vicinity of the critical distance at higher iteration levels.

A method is presented here that makes no supposition as to the quality of the data and takes advantage of several characteristics of seismic refraction data. Because shallow seismic refraction data may be modeled by a series of line segments, many aspects of the general solution of the multisegmented regression problem, as presented by Hudson, may be omitted. The parameters for each line segment, wave slowness and time intercept, are calculated, and under the assumption that the distribution of time values at a distance are normally and independently distributed, the standard deviations of these parameters are found. An algorithm, utilizing Hudson's 2 segment regression analysis, is presented here which extends his method to fit 3 or more regression lines to seismic refraction data. The statistical uncertainties of the parameters for each line segment are used to estimate the uncertainty in the determination of depth.

#### Unconstrained Join Type

Let the  $n$  time and distance pairs form a series in ascending order, and let there be only one time value for each distance, as  $[(t_1, d_1), \dots, (t_n, d_n)]$ . Let the  $t_i$  be the dependent variable, and let the  $d_i$  be the independent variable. Now the set of time-distance pairs may be partitioned into  $m$  sections, where  $j = 1, \dots, m$ , and a simple linear regression equation may be applied to each section of data. Let one of these sections be composed of a series of  $s$  pairs of values  $[(t_g, d_g), \dots, (t_h, d_h)]$ . Here  $s = h - g + 1$ . The model equation for the  $j$ th section of the data is

$$t_i = \alpha_j + \beta_j d_i + \varepsilon_{ij} \quad i = g, \dots, h \quad (1)$$

The line parameters  $\alpha_j$  and  $\beta_j$  are the time-intercept and wave slowness, respectively. The random variables  $\varepsilon_{ij}$  are normally and independently distributed with a mean of zero and variance  $\sigma_j^2$ . Let the sample estimate for the time intercepts be  $E(\alpha_j) = a_j$  and the sample estimate for the wave slowness by  $E(\beta_j) = b_j$ . The estimator of the variance is  $E(\sigma_j^2) = s_j^2$ . The estimator of each  $\varepsilon_{ij}$  is zero, so the  $m$  regression equations are determined by calculating  $(a_1, b_1, \dots, a_m, b_m)$ . Statistical weights could easily be included here, but for the present discussion they have been omitted.

The line segments should be continuously connected at points  $D_j$  which are positioned between the end elements of the partitions. There must also be at least 2 points of data on each segment, then the time estimates are

$$\begin{aligned} \hat{t}_i &= a_1 + b_1 d_i & \text{for } 0 < d_1 < d_2 < D_1 \\ \hat{t}_i &= a_2 + b_2 d_i & \text{for } D_1 < d_i < d_{i+1} < D_2 \\ &\cdot & \cdot & \cdot \\ \hat{t}_i &= a_j + b_j d_i & \text{for } D_{j-1} < d_i < d_{i+1} < D_j \\ &\cdot & \cdot & \cdot \\ \hat{t}_i &= a_m + b_m d_i & \text{for } D_m < d_{n-1} < d_n \end{aligned} \quad (2)$$

For the  $j$ th section of the time-distance series, the deviation of each time value,  $t_i$ , from it's estimation,  $\hat{t}_i$ , is

$$e_{ij} = t_i - a_j - b_j d_i \quad (3)$$

Temporarily let the  $j$ th section of the data be considered separately, as  $[(t_i, d_i) \ i = g, \dots, h]$ . The residual sum of squares from Equation 3 is

$$RSS_j = \sum_{k=1}^s e_k^2 \quad (4)$$

where the length of the  $j$ th section is  $s$ . The following sums must also be calculated.

$$\begin{aligned} Sd_j &= \sum_{k=1}^s d_k & St_j &= \sum_{k=1}^s t_k \\ Sdd_j &= \sum_{k=1}^s d_k^2 & Stt_j &= \sum_{k=1}^s t_k^2 \\ Sdt_j &= \sum_{k=1}^s d_k t_k \end{aligned} \quad (5)$$

Steinhart and Meyer (1961, Eq. 1 and 2) have presented the solution of the line parameters,  $a_j$  and  $b_j$ . They are

$$a_j = \frac{Sdd_j St_j - Sd_j Sdt_j}{sSdd_j - (Sd_j)^2} \quad (6)$$

and

$$b_j = \frac{sSdt_j - Sd_j St_j}{sSdd_j - (Sd_j)^2} \quad (7)$$

Now the variance of the wave slowness is

$$\sigma_j^2(b) = RSS_j / [(s-2)SSd_j] \quad (8)$$

where

$$SSd_j = \sum_{k=1}^s (d_k - \langle d \rangle)^2$$

The angle brackets indicate average. Steinhart and Meyer (Eq. 13) have shown that the variance of the mean value of the regression line at any distance,  $d$ , is

$$\sigma_j^2(d) = \frac{RSS_j}{s-2} \left[ \frac{1}{s} + \frac{(d - \langle d \rangle)^2}{SSd_j} \right] \quad (9)$$

At the time intercept,  $d = 0$ , the variance is

$$\sigma_j^2(a) = (RSS_j/s-2) (1/s + \langle d \rangle^2/SSd_j) \quad (10)$$

Substituting Equation 8 into Equation 10 and using the identity

$$SSd_j = \sum_{k=1}^s d_k^2 - \left( \sum_{k=1}^s d_k \right)^2/s, \quad \text{then} \quad (11)$$

$$\sigma_j^2(a) = [\sigma_j^2(b) SSd_j]/s$$

Equations 4, 8, and 11 may be applied to any section of the data.

The join points  $D_1, \dots, D_m$  represented on the model given by Equation 2 are not constrained to a particular value but may be located anywhere between the uppermost distance  $d_i$  of one segment and the lowermost distance  $d_{i+1}$  of the next segment. Let this type of join, where the data are separated, be called s-join. The total residual sum of squares is

$$RSS_T = \sum_{j=1}^m RSS_j \quad (12)$$

Consider a 2-segment regression ( $r = 2$ ). The computation necessary to find the best statistical fit of 2 lines fitted to the data proceeds by passing a line through  $[(t_1, d_1), (t_2, d_2)]$  without error and regressing a line through  $[(t_3, d_3), \dots, (t_n, d_n)]$ . If the intersection of these 2 lines

is between  $d_2$  and  $d_3$ , then these are a valid pair of regression lines because the regression lines join where the data have been separated. The total regression sum of squares  $RSS_T = RSS_1 + RSS_2$  for this combination of lines. If instead the intersection is not between  $d_2$  and  $d_3$  this combination of lines is rejected as a possible 2-segment regression candidate. Next the first (3) pairs and the last  $(n-3)$  pairs are fitted. Again, if the intersection is found to be between  $d_3$  and  $d_4$  we have an acceptable candidate. The procedure is continued, testing each possible combination of data, to the last combination which is  $[(t_1, d_1), \dots, (t_{n-2}, d_{n-2})]$  and  $[(t_{n-1}, d_{n-1}), (t_n, d_n)]$ . Of these candidates the best statistical fit is the candidate which has the smallest  $RSS_T$ . For  $r = 2$  the total number of combinations that must be tested is  $(n-2)$ .

Hudson (1966, p. 1104) has shown that for those candidates that have not been rejected, the estimates of the regression parameters are valid. After the best statistical fit has been found, the coefficients  $(a_1, a_2, b_1, b_2)$  are calculated from Equations 6 and 7 and their variances  $[\sigma_1^2(a), \sigma_1^2(b), \sigma_2^2(a), \sigma_2^2(b)]$  are calculated from Equations 8 and 11.

If  $r > 2$  then the same basic computational plan would follow, and if all the join points were s-join, the overall least squares solution would be the best fit of  $r$  line segments found as local least squares solutions from all possible combinations of the data points.

#### Constrained Join Type

Although the data have been searched for all s-join candidates, the set of all possible linear regression fits is still not complete. The model regression equations in Equation 2 must also be tested for the case where



the join points are located on time ordinate fixed at the data point distances. This type of join is here called c-join because, for each pair of regression lines, one data point is common to the solution of each line. The system of model equations, with the constraint that the lines join somewhere on ordinate corresponding to  $d_i$ , has been solved with the use of a Lagrange multiplier.

As before, the details of the procedure will be presented for  $r = 2$ . The appropriate linear constraint is that the lines join at some  $D$ .

$$a_1 + b_1 D = a_2 + b_2 D \quad (13)$$

Again let the time-distance pairs be  $[(t_1, d_1), \dots, (t_n, d_n)]$ , and let the c-join be located at  $D = d_\gamma$ . Before the calculations of the residual sum of squares and the coefficients of the line segments are made, a number of sums must be found.

$$\begin{aligned} Sd_1 &= \sum_{k=1}^{\gamma} d_k & Sd_2 &= \sum_{k=\gamma+1}^n d_k \\ Sdd_1 &= \sum_{k=1}^{\gamma} d_k^2 & Sdd_2 &= \sum_{k=\gamma+1}^n d_k^2 \end{aligned} \quad (14)$$

Following Hudson (p. 1126) the terms  $\phi$  and  $\psi$  are

$$\phi = a_1 - a_2 + (b_1 - b_2)D \quad (15)$$

and

$$\psi = \frac{Sdd_1 - 2DSd_1 + \gamma D^2}{\omega_1} + \frac{Sdd_2 - 2DSd_2 + (n-\gamma)D^2}{\omega_2} \quad (16)$$

where

$$\omega_1 = \gamma Sdd_1 - (Sd_1)^2$$

$$\omega_2 = (n-\gamma) Sdd_2 - (Sd_2)^2$$

Let  $RSS_T^*$  be the total residual sum of squares for two line segments connected with a c-join, and from before, let  $RSS_1$  and  $RSS_2$  be the unconstrained residual sum of squares, then

$$RSS_T^* = RSS_1 + RSS_2 + \phi^2/\psi \quad (17)$$

Finally, let  $(a_1^*, b_1^*, a_2^*, b_2^*)$  be the coefficients of the line segments joined by c-join, and let  $(a_1, b_1, a_2, b_2)$  be the unconstrained coefficients as determined from before. The new coefficients are:

$$\begin{aligned} a_1^* &= a_1 - (\phi/\psi\omega_1)[Sdd_1 - DSd_1] \\ b_1^* &= b_1 + (\phi/\psi\omega_1)[Sd_1 - \gamma D] \\ a_2^* &= a_2 + (\phi/\psi\omega_2)[Sdd_2 - DSd_2] \\ b_2^* &= b_2 - (\phi/\psi\omega_2)[Sd_2 - (n-\gamma)D] \end{aligned} \quad (18)$$

A line segment with these coefficients does not pass through its point of mean time and distance.

The computational scheme could proceed from this point by testing the data from  $\gamma = 2, \dots, n-1$  and finding the minimum  $RSS_T^*$ , as had been done for the s-join candidates, but several short cuts may be taken. The complete set of combinations with s-joins may be used to reduce the number of combinations with c-joins. Hudson (1966, Theorem 3) has investigated the case for  $r = 2$ . Each of these combinations may be rejected and not calculated if they pass one of the following 5 tests:

Test 1. At each s-join candidate, say at  $i = \xi$ , the c-join candidate need not be calculated at  $\gamma = \xi, \xi + 1$ .

Test 2. If at any  $i$ ,  $RSS_1 + RSS_2 > \text{Min } RSS_T$  (Minimum  $RSS_T$ ), even if the join point was not between the end members of the 2 sets of data, the c-join candidate need not be calculated at  $\gamma = i, i+1$ .

At this point the static tests for the elimination of possible c-join candidates have been exhausted, and the calculation of  $RSS_T^*$  must be made at c-join locations from  $\gamma = 3, \dots, n-2$ . After each calculation of  $RSS_T^*$  through, the next 2 dynamic tests should be made to further reduce the number of possible c-join locations.

Test 3. Let a  $RSS_T^*$  be calculated and from these let a  $\text{Min } RSS_T^*$  be found. If at any  $i$ ,  $RSS_1 + RSS_2 > \text{Min } RSS_T^*$ , even if the join was not located between the end members, then the c-join candidate need not be calculated for  $\gamma = i, i+1$ .

Test 4. Let a  $RSS_T^*$  be calculated at some  $\gamma$  and that the mean distances for the left and right line segments are found as  $\langle d_l \rangle = Sd_1/\gamma$  and  $\langle d_r \rangle = Sd_2/(n-\gamma)$ . If the join point  $D$  from the s-join calculations is  $\langle d_l \rangle < D < \langle d_r \rangle$  then  $RSS_T^*$  need not be calculated at any  $\gamma$  such that  $\langle d_l \rangle \leq d_\gamma \leq \langle d_r \rangle$ .

Finally a test at  $\gamma=2$  and  $\gamma = n-1$  is presented.

Test 5. At  $\gamma = 2$  and  $\gamma = n-1$ , regression lines may be fitted and residual sum of squares,  $RSS_2$  and  $RSS_{n-1}$ , may be calculated on the data sets  $[(t_2, d_2), \dots, (t_n, d_n)]$  and  $[(t_1, d_1), \dots, (t_{n-1}, d_{n-1})]$ , respectively. Then a second regression line may be drawn through  $(t_1, d_1)$  and the intersection of the first regression line with  $d_2$  (without error). Similarly a second regression may be drawn through  $(t_n, d_n)$  and the intersection of the second regression line with  $d_{n-1}$ . If  $RSS_2 > \text{Min } RSS_T$ , then  $RSS_T^*$  at  $\gamma = 2$  need not be calculated. And if  $RSS_{n-1} > \text{Min } RSS_T$ , then  $RSS_T^*$  at  $\gamma = n-1$

need not be calculated.

At this point for  $r = 2$ , all  $(n-3)$  calculations have been completed for the s-join candidates, and of these, the 2-segment candidate with  $\text{Min RSS}_T$  has been retained. There are  $(n-2)$  possible candidates with c-join, and hopefully, many of these have been rejected by the tests. From those that were calculated, the c-join candidate with  $\text{Min RSS}_T^*$  has also been retained. There are then a total of  $(2n-5)$  possibilities for  $r = 2$ . The final least squares solution is either the minimum s-join candidate or the minimum c-join candidate, whichever has the smaller residual sum of squares.

As before when  $r > 2$ , the same basic computational scheme would be followed for the search for c-join candidates. It is not surprising that the total number of possible candidates grows rapidly for problems involving many segment models or large sets of data, although many may be rejected by the tests. When  $n = 24$  and  $r = 2$  the number of possible candidates is 43, and when  $n = 24$  and  $r = 3$  the total is 841. For greater  $n$  or  $r$  the number of possible candidates is extremely large. For example, when  $n = 100$  and  $r = 6$  the total number of possible candidates is near  $1.9 \times 10^9$ .

#### An Algorithm

Seismic refraction measurements provide data which are sufficiently linear to allow certain liberties in the curve-fitting process. The first of these is to suppose that some reasonable estimate may be made of the maximum number of permissible line segments present in the investigation. The estimate does not need to be known, but that only some upper limiting number may be chosen.

This decision though must be tempered with the inherent tendency for

higher-numbered regression systems to fit the data better than lower-numbered systems. To be guided in this direction, one must choose a value high enough so that no line segment is missed, but not so high that the curve is 'over-fitted' and the solution is physically impossible. This would be the case when the fitted solution contains velocity reversals. The second criterion then is that starting from the origin, the velocity of each line segment must monotonically increase. In practice, this is a valuable guide to the selection of the best least squares solution.

In a 2 segment linear regression model, the residual sum of squares may be plotted against join point distance. In the limit as  $n \rightarrow \infty$  the residual sum of squares form a curve, and the minimum point on this curve corresponds to the distance at which the two regression lines intersect. For a 3 segment linear regression as  $n \rightarrow \infty$  the best least squares solution is the minimum point on a surface of residual sum of squares. This surface is formed on 2 axes which correspond to the  $D_1$  and  $D_2$  join point values and a third axis which is the residual sum of squares. The analogy is similar for more line segments. If this  $r$ -dimension surface is reasonably simple, the minimum point may be reached by making a series of traverses across the surface, each of which is accomplished by varying the values of only one join point. Each traverse is equivalent to the 2 segment regression problem considered earlier.

To evaluate an  $r > 2$  regression system, a number of points along the data must be chosen to effectively lower the number of possible candidates to be searched at any one time to  $(2n-5)$ . These test points should be chosen as near as possible to the suspected join points, but it is preferable to choose them slightly below the suspected join point. In this way no

data points from the next higher line segment enter the calculation. The procedure advances by searching for 2 segment joins in successive sets of data. Each successive set of data has an upper bound which has been set by a test point and a lower bound which has been set at the join point found in a preceding join search.

As an example, suppose there are 3 suspected line segments to be fitted to time-distance pairs where  $[(t_i, d_i) \ i = 1, \dots, n]$ . There must be 1 test point chosen at or slightly below the suspected join between the second and third line segments, say at  $i = T$ . The pairs  $[(t_i, d_i) \ i = 1, \dots, T]$  are first searched for the join between the first and second line segment. Let the solution for this set of data be an s-join candidate between  $i = \zeta$  and  $i = \zeta + 1$ , as  $d_\zeta < D_1 < d_{\zeta+1}$ . The data  $[(t_i, d_i) \ i = \zeta+1, \dots, n]$  is now searched for the join between the second and third line segment. Suppose the solution here is a c-join candidate such that  $d_n < D_2 < d_{n+1}$ . The final solution is composed of 3 line segments joined at  $D_1$  and  $D_2$ , and the total residual sum of squares is equal to the sum of the residual sum of squares from each line segment.

If the solution in the first search had been a c-join candidate the data in the second search would be scanned from  $[(t_i, d_i) \ i = \zeta, \dots, n]$ . Or if a join point had not been found in the first search the data in the second search would have been scanned from  $[(t_i, d_i) \ i = 1, \dots, n]$ , and only a 2 segment solution would have been found. The computation for each search would proceed accordingly.

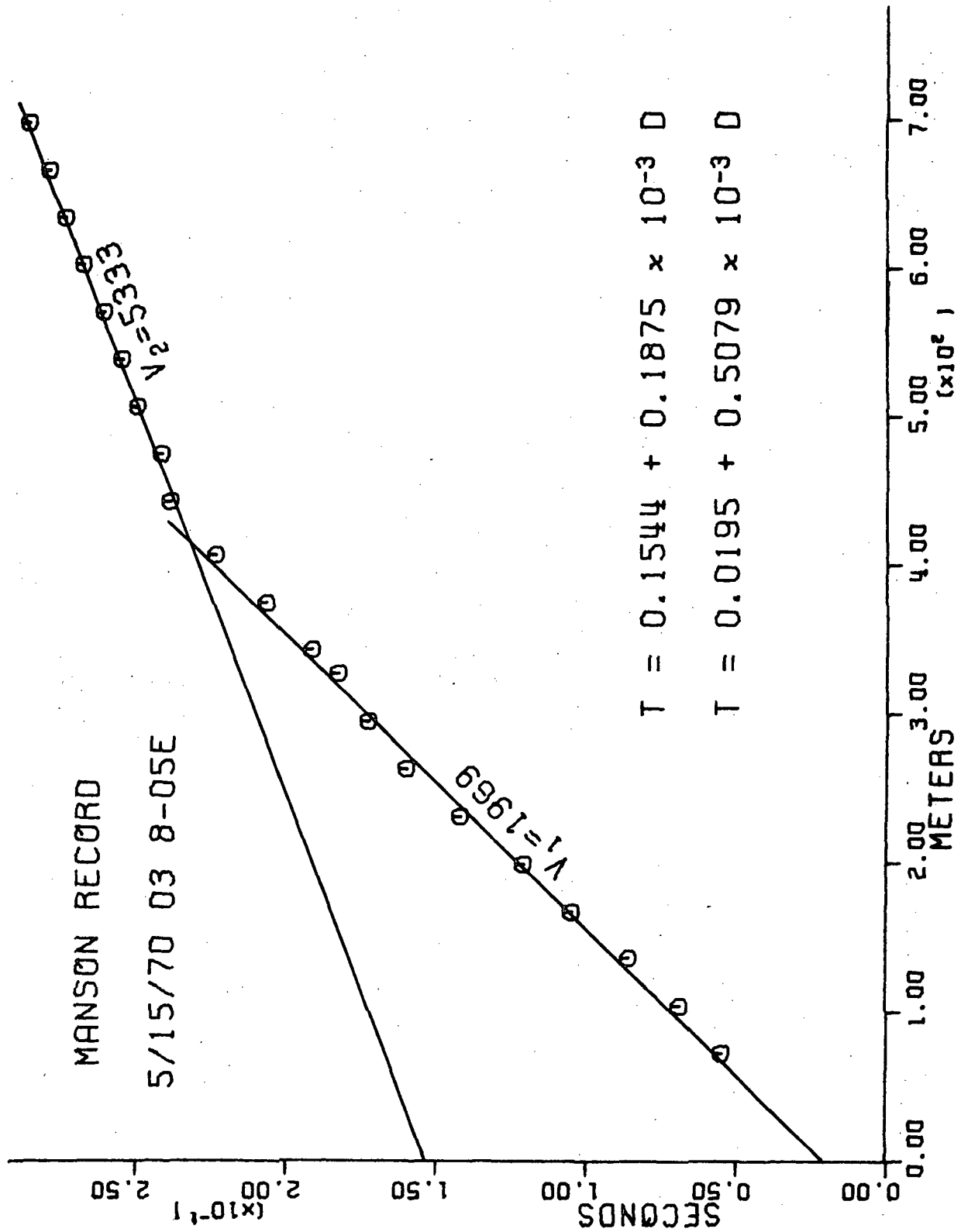
For an n-segment linear regression a vector of test points must be chosen as  $(T_1, \dots, T_{n-2})$  and the algorithm proceeds with  $(n-1)$  levels of 2 segment join search. Because the number of possible candidates to be

searched at each level of join point selection is restricted to the search for a 2 segment fit, the actual computation is greatly reduced.

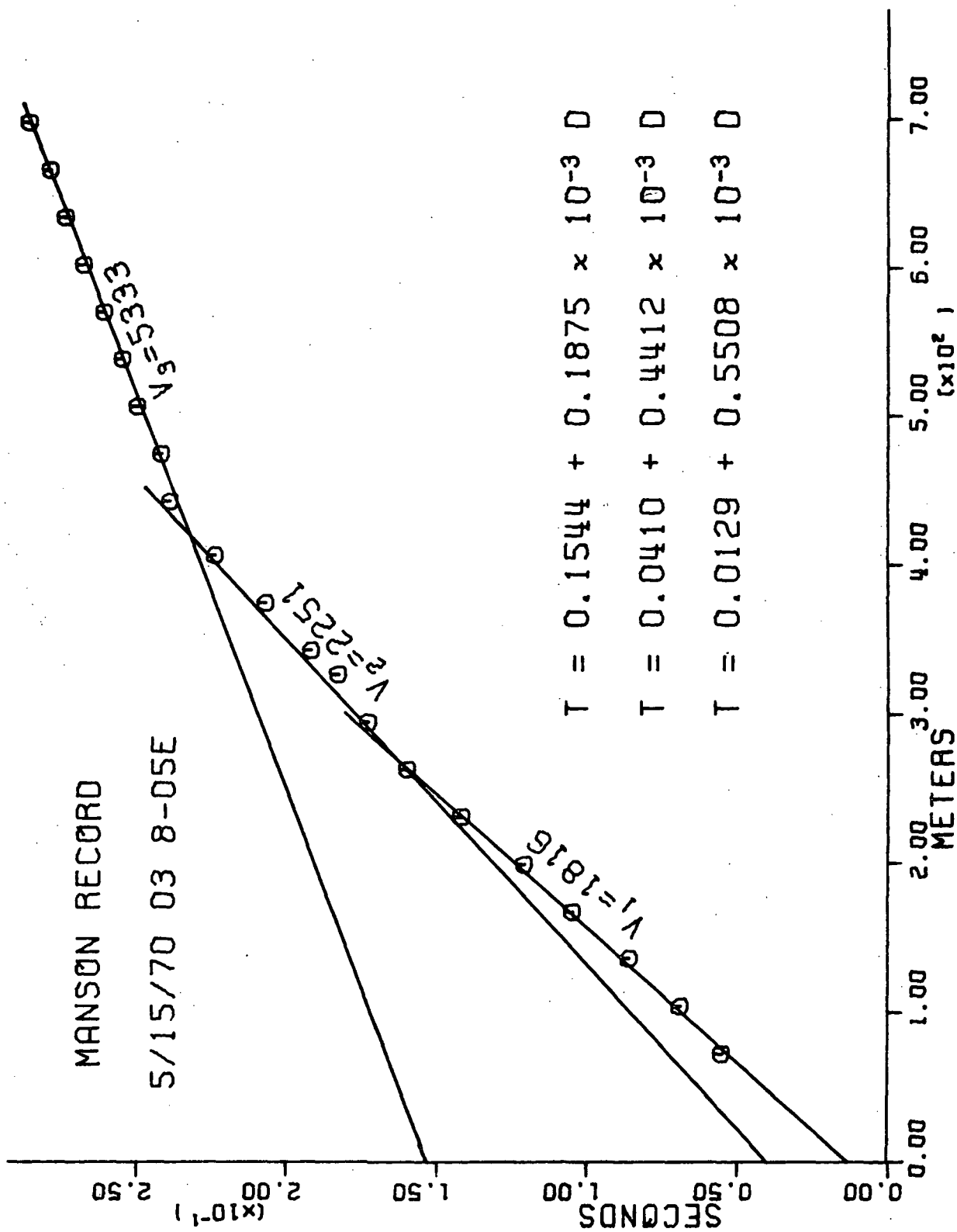
### Examples

An example of a set of data from a typical shallow refraction shot is presented in Figure 4. Here  $[(t_i, d_i) \ i = 1, \dots, 21]$ . A linear regression with all 21 data points yields a line with a velocity of 2682 m/sec and a residual sum of squares of  $0.47325 \times 10^{-2} \text{ sec}^2$ . The best s-join candidate from a 2 segment regression analysis is superimposed on the data in the figure. The join point is located at a distance of 421 m and the total residual sum of squares is  $0.13222 \times 10^{-3} \text{ sec}^2$ . All possible c-join combinations were eliminated by the 5 tests, so the s-join candidate is the best overall 2 segment regression fit.

The best 3 segment regression is presented in Figure 5. A test point at  $d_8$  was chosen, and a 2 segment analysis of  $[(t_i, d_i) \ i = 1, \dots, 8]$  revealed that the best fit was a c-join candidate joined on the time ordinate corresponding to  $d_2$ . The second level of data then consisted of  $[(t_i, d_i) \ i = 2, \dots, 21]$ . The best statistical fit here was an s-join candidate with a join between  $d_{12}$  and  $d_{13}$ . To be sure the test point was correctly chosen, the set  $[(t_i, d_i) \ i = 1, \dots, 12]$  was analyzed. This time the best fit was a c-join candidate with join point at  $d_7$ . This third scan of the data protected the overall solution from an inaccurate choice of test point. Here the test point of  $d_8$  was too low and should have perhaps been  $d_{12}$ . The overall 3 segment regression fit has a total residual sum of squares of  $0.44170 \times 10^{-4} \text{ sec}^2$ . A borehole adjacent to the shot showed that the 3 segment fit compared favorably in velocity and depth with glacial drift,







shale, and limestone.

These two examples show that two valid regression models may be fitted to the shallow seismic refraction data. At other times only a 2 segment regression model may be acceptable. This situation might arise if the 3 segment regression model contained a velocity reversal between two adjoining line segments. In the first case additional information must be used to discriminate between the two cases. This information is acquired from a knowledge of the geological conditions in the area.

## ANALYSIS OF NEAR-SURFACE VELOCITIES

Multi-layered earth models of any dimension, whether they are based on bedrock structures measured in meters or crustal structures measured in kilometers, may be developed from seismic refraction data only when velocity measurement of the uppermost layer has been made. On many scales the earth may be approximated by a model bounded by a series of planar surfaces. The compressional wave velocity of this uppermost earth material may, in theory, be calculated from the reciprocal of the slope of a line segment that passes through the origin of the time-distance graph of the data.

## Selection of Data

Many seismic refraction investigations are hampered by a lack of knowledge of the near-surface geologic environment near the shot and under each geophone. In shallow refraction investigations the plot of some records reveals that perhaps one or two data points nearest the shot fall markedly below the first fitted line segment. They may represent random scatter about the first line segment, or they may represent travel times from direct waves passing through a shallower layer. In either case, the first layer is not detected because there is a lack of data from each record due to the fixed sampling intervals along the distance axis at which time was measured. By combining the data from all records the lack of data at near distances on individual records is overcome, and the maximum times in each interval may be used to estimate the minimum velocity of the first detected layer of a generalized model for the entire study area.

In the Manson area, line segments drawn through the first several time distance points on each shot record did not pass through the origin, so the

entire set of first arrival time-distances pairs was plotted. The field of points is shown on the scatter diagram (Figure 6). The locus of points near the time axis clearly demonstrates that the first layer line segments do not pass through the origin. Although the lower border of data scatter is not well marked, the upper border is strikingly smooth.

In an endeavor to better understand the nature of this upper border, the distances of all time-distances pairs were partitioned with a class interval of 5 m, as 0-5 m, 5-10 m, etc., and the corresponding time values in each interval were scanned for the maximum time in each interval. A plot of these maximum time values was found to be quite regular even to a distance of 500 m from the origin. The maximum time at this distance was 0.275 sec. The scatter of the maximum times beyond 500 m is probably due to the smaller sample sizes in each interval at these farther distances.

It was found that the locations of these time-distance pairs which had a maximum time were uniformly scattered over the entire area. The original records, from which these time values were taken, were then reexamined to see if these times might have been taken from traces where the refracted wave was obscured or where the arrival time was incorrectly measured. Because of the large size of the shot charges, first arrival onsets were quite strong even at the farthest recording distances. It is unlikely that the maximum time values could be attributed to poor record quality or to second arrivals from later phases, particularly for distances less than 500 m.

#### Statistical Analysis

Once that it had been established that the maximum time values were valid refraction arrival times, these maximum time-distance pairs were

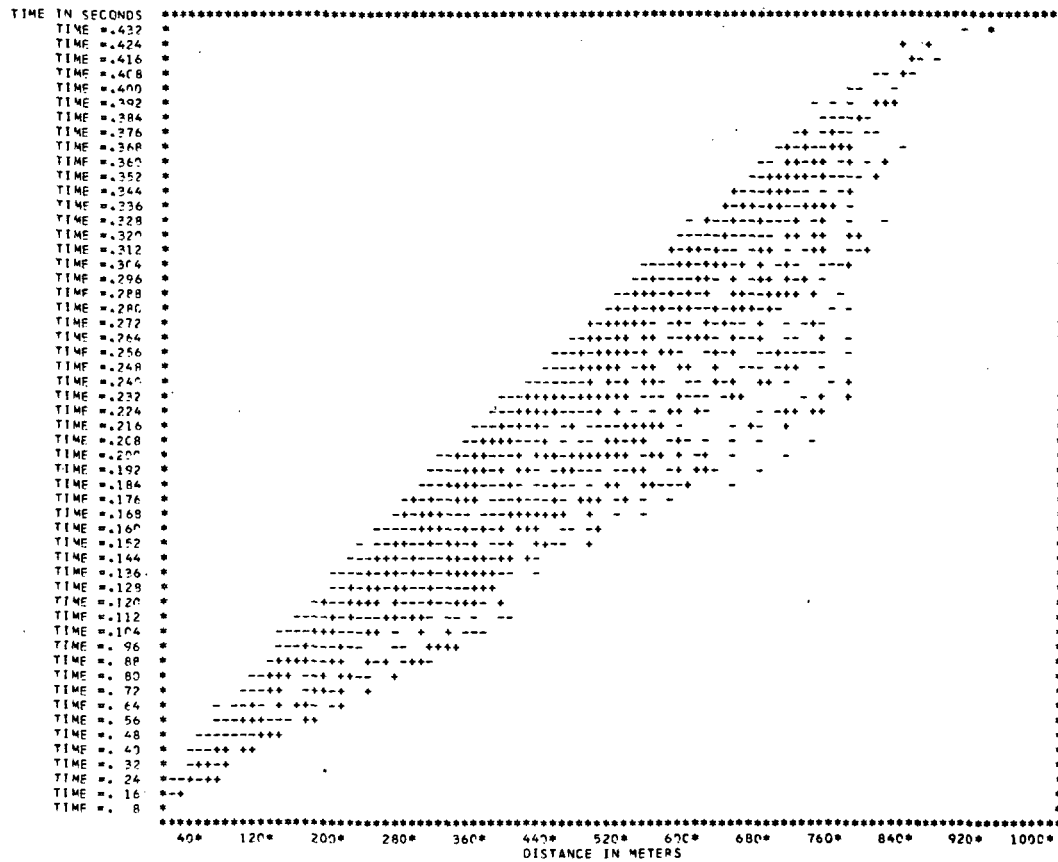


Figure 6. Scatter diagram of all time-distance measurements

statistically fitted with line segments as if they were data from a single seismic record as described previously. By this method a portion of the set of all possible combinations of linearly regressed line segments was searched for the one fit which had the minimum residual sum of squares. The first 100 time-distance pairs were fitted with 1, 2, 3, and 4 line segments. The results are tabulated in Table 1. The first line segment from the 4 segment model best fits the maximum time values at the nearest distances. Models with a greater number of line segments suffered from velocity reversals in the first and second line segments, probably due to random deviation of the maximum time values and accentuated by the fewer number of points represented on the first fitted line segment.

Table 1. Statistical fits of first 100 maximum times

Model	Points	Velocity <sup>a</sup>	Residual sum of squares <sup>b</sup>
1 layer	100	1919	0.24530
2 layer	53	1771	0.12464
	47	2138	
3 layer	12	1462	0.10938
	50	1844	
	38	2203	
4 layer	7	1258	0.10772
	20	1749	
	40	1863	
	35	2200	

<sup>a</sup>In m/sec.

<sup>b</sup>In  $10^{-2}$  sec<sup>2</sup>.

From the analysis of the data collected at Manson, it is inferred that the minimum velocity of the first detected layer is near 1250 m/sec. A line with a slope corresponding to a layer with velocity of 1250 m/sec may not be made to pass through the origin and still remain within the data scatter. Therefore, the first layer has not been detected, for if it were, the line with a velocity of 1250 m/sec would pass through the origin.

Several investigators (Hobson, 1969; Staub, 1969) have suggested that at very short distances, the first detected energy arrives at the geophone from a ground-coupled air wave when the velocity of the surficial layer is less than the velocity of sound. Although the detection of this air wave was not an object of the present study, all depth calculations in this study include a first line segment which is attributed to a ground-coupled air wave. To avoid confusion the first statistically fitted layer has been called the first layer. The depth to the '"air" - first layer' interface has been found to range from 1 to 2.5 m.

## ANALYSIS OF DEEPER VELOCITIES

The velocity determinations from the statistical line-fitting analysis of individual seismic records may be combined to indicate the variability of the velocities of various seismic refractors. The utility of the shallow seismic refraction technique rests not on the analysis of each seismic record, but on how well seismic refractors may be traced below many seismic stations, and how well the depths to the seismic refractors compare with lithologic changes at depth, as indicated from borehole data.

### Statistical Analysis

Nineteen seismic spreads were placed as near as possible to boreholes where adequate well logs were available, so that a correlation between seismic refractor layers and lithologic units could be established. These records were plotted and analyzed with the statistical line fitting method mentioned previously. Test points were chosen as near as possible to the join between suspected second and third line segments. Each seismic record was fitted with 2 and 3 line segments.

The uniqueness of the statistical fit depends on the choice of test points. In an attempt to improve the 3 line segment fits, each record was analyzed with a variety of test points. The final statistical fit of the data for the 3-layer model does not seem to be very sensitive to the location of the test point. Experience on artificially generated 3-layer data has shown that if the test point is chosen between the middle of the second line segment and the join point between the second and third lines segments, a correct solution is found.

The statistical fitting method was also measured by how well it



eliminated the number of calculations of 2 segment regressions. For any particular set of  $n$  time-distance pairs, the search for the best fit of 2 line segments joined between data points (s-join) was necessarily applied to all  $(n-3)$  combination of data points. The robustness of the 5 tests used to eliminate the calculation of the regressions of 2 line segments connected with a c-join was measured by the percentage of calculations that had been eliminated. Of the  $(n-2)$  possible combinations to be tested for c-join, approximately 90% could be eliminated from consideration for any one of the 5 tests. The rejection rate for each of the 5 tests was approximately: test 1 - 0%, test 2 - 50%, test 3 - 40%, test 4 - 2%, and test 5 - 8%.

After the validity of the statistical method had been tested, rough correlations were made between model velocities and the borehole lithologies. Test points based on those correlations were then picked on plots of seismic profiles without well log control. These seismic records were then analyzed for both 2 and 3 line segments. In no instance could 4 line segments be satisfactorily fitted to the data because no more than 24 data points were available for each statistical analysis. After the best statistical fits had been made it was necessary to decide, for each record, whether the 2 layer or 3 layer model best fit the geologic conditions.

### Velocity Distributions

The final results are plotted on Figure 7. The frequency polygons for the first layer velocities, second layer velocities, and a combination of first, second, and third layer velocities are plotted with the distance axis divided by a class interval of 50 m/sec. The results are plotted at the

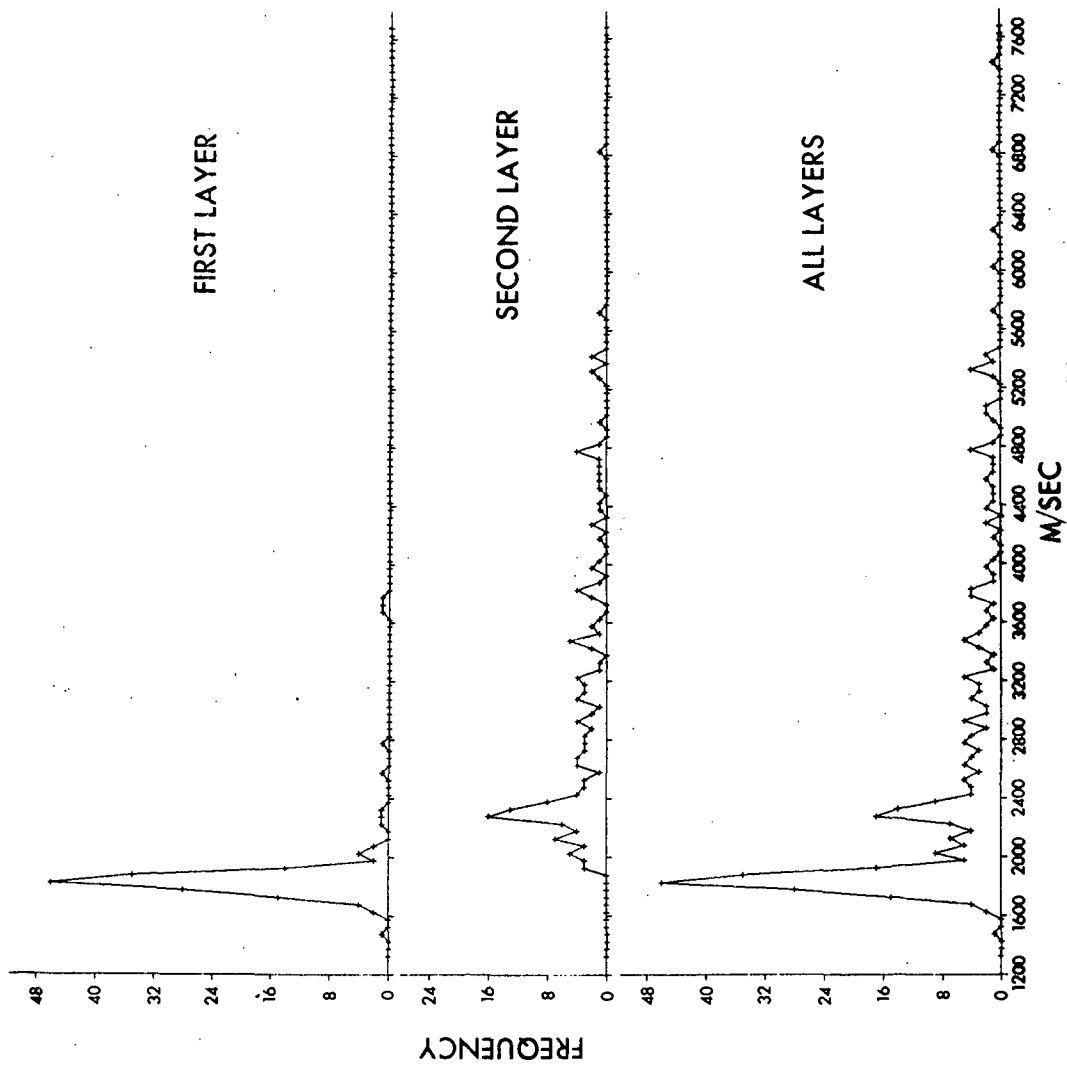


Figure 7. Distribution of seismic velocities by Layer

mid-point between the ends of the class intervals.

The narrow distribution of first layer velocities is attributed to glacial drift. Much of the velocity of the glacial drift is between 1800 and 1850 m/sec. It is significant to note that the distribution about the main peak is symmetric. This indicates that there is only one type of material measured in the distribution. The presence of a second material with a slightly higher velocity, for example the disturbed shale, would skew the distribution to the right. The presence of a second material with a slightly lower velocity would accordingly skew the distribution to the left. The shape of the main first layer distribution compares favorably with the velocity distribution of other glacial drifts as presented by Hobson (1969), Lennox and Carlson (1969) and Staub (1969). The several first layer velocities above 3600 m/sec were from seismic stations on the eastern portion of the area in the undisturbed area where the glacial drift was known to be quite thin.

The frequency of velocities between 2250 and 2300 m/sec on the second graph is the highest on the plot. The distribution is not nearly as sharp as the glacial drift distribution in the first layer but it represents a portion of the disturbed shale velocity distribution. Superimposed on this graph are the velocities of the undisturbed bedrock layers which include undisturbed limestones and dolomites ranging in velocity from 3000 to 7000 m/sec and the velocity of the crystalline bedrock which ranges from 3000 to 5000 m/sec.

As an example of the irregularity of the bedrock velocity, at station 6-13E, situated parallel to the rim of the Manson disturbed area, a 24 trace record shooting north yielded first, second, and third layer velocities of

1761, 3982, and 5360 m/sec. The second shot detonated between the cables produced records in both the north and south direction. For the north spread, layers of 2061 and 5417 m/sec were detected and for the south, layers of 1762 and 4540 were found. The west end of station 6-14E was adjacent to the south end of station 6-13E. Here, the west spread detected layers of 1595 and 4764 m/sec, and the east spread detected layers of 1679, 3077, and 6275 m/sec. It may be seen that neither the second or third layer may be easily correlated with any other layer on any other record.

The graph of the combined distributions from the first, second, and third layer reflects all the features mentioned previously. The few points added at higher velocities are from deeper refracting horizons in the carbonate sequence of bedrocks in the eastern undisturbed area. Both the disturbed and undisturbed velocity distributions are suspect of being quite scattered.

## VELOCITY CONSIDERATIONS

The velocity distributions are not a true representation of the velocities of the seismic refractors. The presence of dipping refractors, velocity anisotropy, velocity reversals, hidden layers, and inadequate velocity contrast will affect, in varying degrees, the measurement of seismic velocity. Each will be considered in this order.

### Dipping Refractors

At nearly all locations the shooting pattern was such that travel times in opposite directions were recorded. In the split spread configuration, where the shot was detonated between the two geophone cables, the travel times represent samples of data collected from separate geologic settings, and in the reverse profile configuration, where shots were detonated near the far ends of the cables, the travel times represent samples of data collected from one geologic setting. The split spread configuration will then produce 2 seismic records based on 2 separate sections of material, and the 2 velocities, taken from the first line segments in each record, may be compared. Similarly, the velocities, taken from the second line segments in each record, may be compared, and so on. The reverse profile configuration also allows these velocity comparisons to be made and further allows a check to be made on travel time reciprocity.

These two tests must be applied to each pair of line segments from corresponding records before the dip calculations may be made. These tests have not, to the authors knowledge, been suitably framed in statistical analysis as they must, if the validity of the ultimate results are to be considered in the light of error of measurement. The statistical tests of

coefficients for several regression lines is a topic of analysis of covariance, and may be found in many books on linear regression, for example Wine (1964).

First consideration must be given to the question whether the slopes,  $b_1$  and  $b_2$ , of each pair of corresponding line segments are statistically different. If there is no statistical difference between the slope estimates, they may be combined, and one slope value may be computed for that pair. If they are different, then a valid pair of slopes whose reciprocals are apparent dip velocities may be analyzed.

Following Wine (1964, p. 554), 2 true model equations, based on separate sets of time-distance data, may be written as

$$t_{1i} = \alpha_1 + \beta_1 d_{1i} + \epsilon_{1i} \quad \text{where } i = 1, \dots, n_1 \quad (19)$$

$$t_{2i} = \alpha_2 + \beta_2 d_{2i} + \epsilon_{2i} \quad \text{where } i = 1, \dots, n_2$$

The least-squares estimators of  $\alpha_1$ ,  $\alpha_2$ , are  $a_1$ ,  $a_2$ , and the estimators of  $\beta_1$ ,  $\beta_2$  are  $b_1$ ,  $b_2$ . Now under the assumption that  $\epsilon_{1i}$  and  $\epsilon_{2i}$  are normally and independently distributed with mean zero and constant variance  $\sigma_1^2$  and  $\sigma_2^2$  at any point on each regression line, the estimated regression of time on distance is

$$\begin{aligned}\hat{t}_{1i} &= a_1 + b_1 d_{1i} \\ \hat{t}_{2i} &= a_2 + b_2 d_{2i}\end{aligned}\tag{20}$$

because the expectation of the random component of each equation is zero.

Let the terms  $e_1$ ,  $e_2$  be the measure of deviation at each  $d_i$  for each regression line in Equation 19 and are given as

$$\begin{aligned}e_{1i} &= t_{1i} - a_1 - b_1 d_{1i} \\ e_{2i} &= t_{2i} - a_2 - b_2 d_{2i}\end{aligned}\tag{21}$$

These are, in a sense, a measure of randomness at each  $d_i$  for each regression line. The residual sum of squares of Equations 21 are

$$\begin{aligned}RSS_1 &= \sum_{i=1}^{n_1} e_{1i}^2 \\ RSS_2 &= \sum_{i=1}^{n_2} e_{2i}^2\end{aligned}\tag{22}$$

The test of the equivalence of 2 slope parameters is stated as the hypothesis  $H_0: \beta_1 = \beta_2 = \beta_0$ . Under the null hypothesis that  $\beta_1 - \beta_2$  is normally distributed and the common population variance is unknown, the statistic  $\tau$  is given by

$$\tau = \frac{b_1 - b_2}{s[(1/SSd_1) + (1/SSd_2)]^{1/2}}\tag{23}$$

where

$$SSd_1 = \sum_{i=1}^{n_1} (d_{1i} - \langle d_1 \rangle)^2$$

$$SSd_2 = \sum_{i=1}^{n_2} (d_{2i} - \langle d_2 \rangle)^2$$
(24)

and the pooled estimate of variance  $s^2$  in Equation 23 is

$$s^2 = \frac{RSS_1 + RSS_2}{n_1 + n_2 - 4}$$
(25)

Now instead of applying Equation 8 to segments of one regression analysis, let it be applied to these 2 regression lines from separate records.

$$SSd_1 = RSS_1 / [(n_1-2) \sigma_1^2(b)]$$

$$SSd_2 = RSS_2 / [(n_2-2) \sigma_2^2(b)]$$
(26)

The statistic  $\tau$  is

$$\tau = \frac{b_1 - b_2}{\left\{ \left[ \frac{RSS_1 + RSS_2}{n_1 + n_2 - 4} \right] \left[ \frac{(n_1-2) \sigma_1^2(b)}{RSS_1} + \frac{(n_2-2) \sigma_2^2(b)}{RSS_2} \right] \right\}^{1/2}}$$
(27)

The  $\tau$  is distributed with  $n_1 + n_2 - 4$  degrees of freedom.

After  $\tau$  has been calculated it can be compared with the Student's  $t$ , here labeled  $\tau$ , with the same degree of freedom and an appropriate level of significance. If  $\tau$  is greater than Student's  $\tau$  the hypothesis is rejected, and it is concluded that  $b_1$  and  $b_2$  are indeed different.

If the hypothesis cannot be rejected, the pooled estimate of  $\beta$  is given as



$$\langle b \rangle = \frac{SSd_1 - b_1 + SSd_2 - b_2}{SSd_1 + SSd_2} \quad (28)$$

and  $\langle a_1 \rangle$  and  $\langle a_2 \rangle$  are

$$\langle a_1 \rangle = \langle t_1 \rangle - \langle b \rangle \langle d_1 \rangle \quad (29)$$

$$\langle a_2 \rangle = \langle t_2 \rangle - \langle b \rangle \langle d_2 \rangle$$

In this case the analysis may not proceed to the second test with this particular pair of line segments.

As an example of an analysis of slope differences, consider the case where two records from a reverse profile configuration had been best fitted with 3 line segments. The 2 first line segments would be tested to see whether or not there was a significant difference between the slopes. Then the 2 second line segments would be tested to see whether or not there was a significant difference between these slopes. And finally, the 2 third line segments would be tested.

A fundamental criteria in seismic refraction is that opposite ended shots and receivers may be interchanged without affecting the travel times, in other words, they are reciprocal. From this, each pair of line segments crossing the opposite-intercept must have the same time value. To reduce this to a statistically convenient question, the line segments from a hypothetical reversed profile are replotted on one set of axes. Then in an n-layer case, the first line segments should superimpose, and the second to the nth matched pair of line segments should each intersect at a distance S from the origin, which is equal to the shot point to shot

point distance.

Now by shifting the time axis to a new time axis at distance  $S$ , the second to the  $n$ th matched line intersect on this axis. The regression equations then become

$$\begin{aligned} t_{1i} &= a_1 + b_1 S + b_1 d_{1i} \\ t_{2i} &= a_2 + b_2 S + b_2 d_{2i} \end{aligned} \quad (30)$$

By shifting axis, the data are simply coded, and no statistical changes have been made. The statistical test that the two regression lines intersect at this new axis is  $H_0: a_1 + b_1 S = a_2 + b_2 S$ . The statistic  $\tau$  is then stated as

$$\tau = \frac{a_1 - a_2 + S(b_1 - b_2)}{s [(Sdd_1/n_1 Sdd_1) + (Sdd_2/n_2 Sdd_2)]^{1/2}} \quad (31)$$

where  $Sdd_1 = \sum_{i=1}^{n_1} d_{1i}^2$  and  $Sdd_2 = \sum_{i=1}^{n_2} d_{2i}^2$ . As was done with Equation 8, Equation 11 may be rewritten in terms of 2 regression lines from separate records as

$$\begin{aligned} Sdd_1 &= n_1 \sigma_1^2(a) / \sigma_1^2(b) \\ Sdd_2 &= n_2 \sigma_2^2(a) / \sigma_2^2(b) \end{aligned} \quad (32)$$

Then by substituting the Equations 32 into Equation 31, the statistical  $\tau$  is

$$\tau = \frac{a_1 - a_2 + S(b_1 - b_2)}{\left\{ \left[ \frac{RSS_1 + RSS_2}{n_1 + n_2 - 4} \right] \left[ \frac{(n_1 - 2)\sigma_1^2(a)}{RSS_1} + \frac{(n_2 - 2)\sigma_2^2(a)}{RSS_2} \right] \right\}^{1/2}} \quad (33)$$

As before, the calculated  $\tau$  is compared with Student's  $\tau$  with  $n_1 + n_2 - 4$  degrees of freedom at an appropriate level of significance. If the  $\tau$  is greater than Student's  $\tau$ , the hypothesis that the two regression lines intersect at distance  $D$  is rejected, and therefore, there is a significant difference in the opposite intercept times. If the hypothesis cannot be rejected, then there is no significant difference in the opposite intercept times.

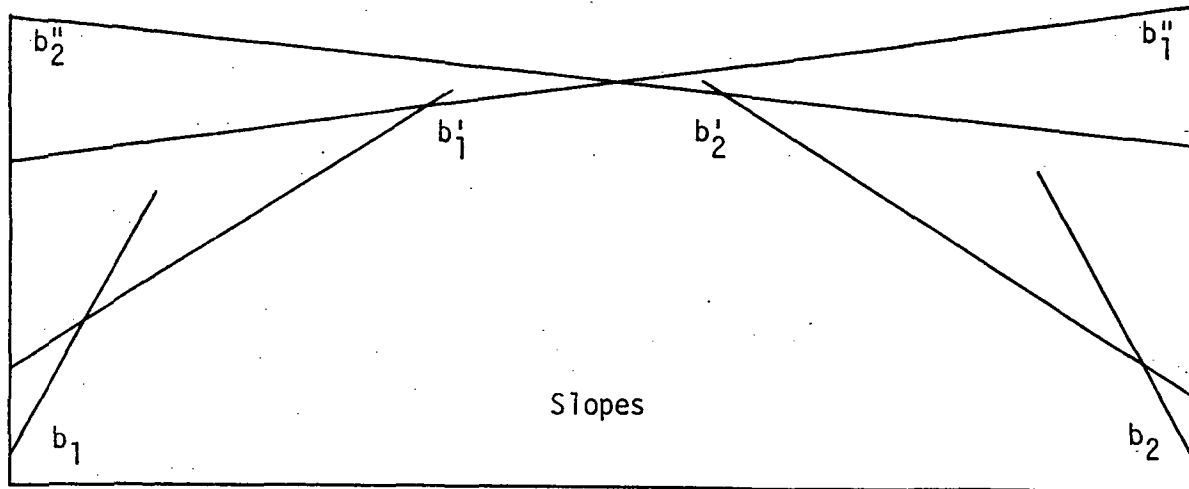
Because the data from split spread profiles were collected from different geologic settings, only the test of slope may be applied. And where reverse profile coverage is available, dip may be calculated on the top of the second layer only when (1) there is no significant difference in the slopes of the first layer, (2) there is a significant difference in the slopes of the second layer, and (3) there is not a significant difference in the opposite-intercept times of the second line segments.

The line segment pairs for each seismic location were tested for slope and opposite-intercept criteria. Unfortunately when the least square fits were calculated only the combined residual sum of squares was retained for those line segments connected by a c-join. Therefore no estimate of the residual sum of squares for the left and right hand line segments was retained. Because of this, neither test of covariance could be applied to any combination of lines where one of the lines did not have a calculated

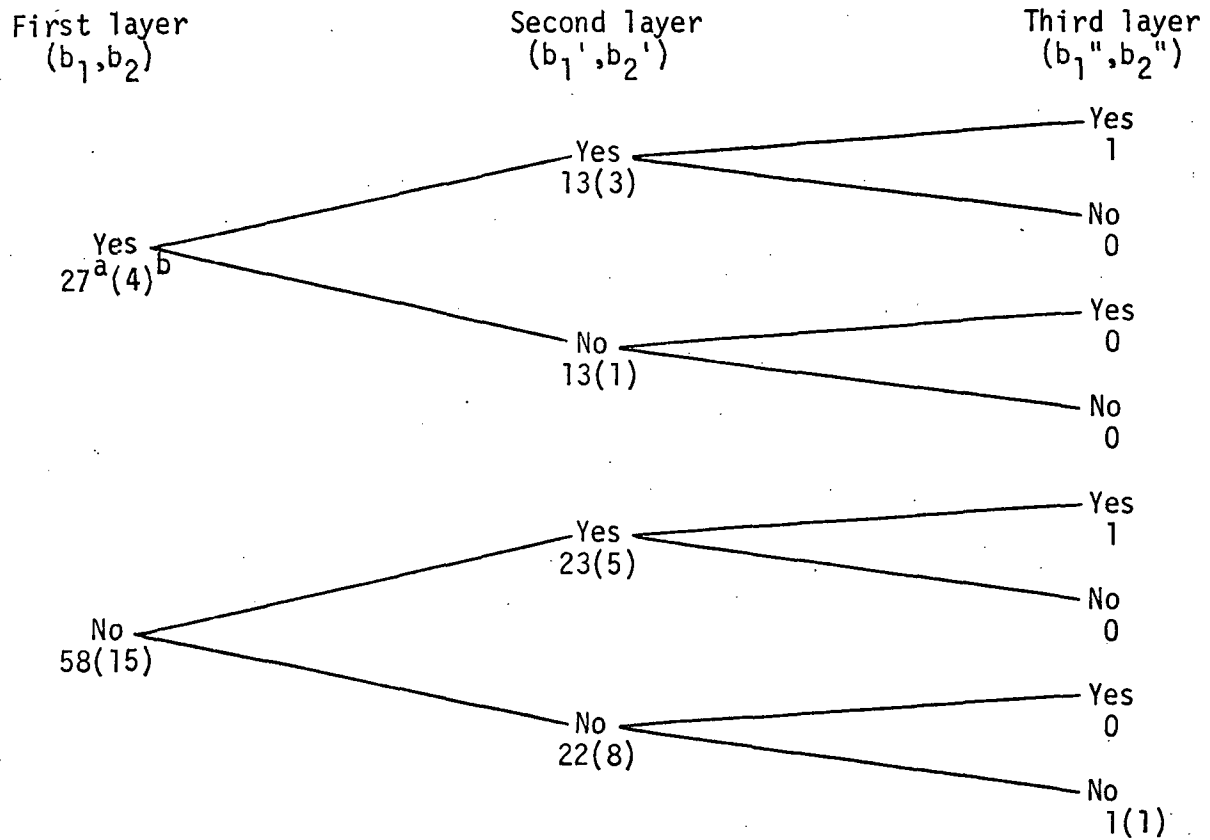
residual sum of squares. Also rejected from consideration were those line segments which had been fitted through only two points.

The results of the slope test are shown on Figure 8. A significant difference in slope was inferred at the 90% confidence level, or simply that there was at least a 90% chance that there was a true difference in slope. Of the stations tested for slope difference, there were approximately 30% (27) where there was a significant difference in the first velocity and approximately 70% (58) where there was not. The results have been drawn in the form of branches to show the different possible cases. Dip calculations on a 2-layer model could only be made on those sites where there was not a sufficient difference in the slopes of the first layer, but where there was a sufficient difference in the second layer. Where no differences were found in either the first or second layer slopes, a horizontal interface model was assumed. This does not imply that the interface is truly horizontal, but that the magnitude of the subsurface undulations of the interface are of such a sufficiently low relief that the time deviations due to this surface have been combined with the error of measurement of time so that the model is simply a plane passing through the average depth to this surface. It is interesting to note that only 23 stations passed the slope criteria for the 2-layer dipping model, and of these, only 1 case could be tested for dip of both the second and third layers.

The results of the opposite-intercept test of the 23 sites that had passed both first and second layer slope tests is presented in Table 2. As in the slope test, a significant difference in opposite-intercept times was inferred as there was at least a 90% chance that there was a true



Significant difference in slopes



<sup>a</sup>Total of all stations.

<sup>b</sup>Station with good borehole control.

Figure 8. Slope test of all seismic sites by line segment

Table 2. Opposite-intercept test of 23 sites that had passed 2-layer slope test for a 2-layer dipping layer model

Seismic site	Shot no.	Significant difference	Relation to Manson disturbed area		
			Outside	Edge	Inside
2-2W	1+2	Yes			
3-3E	3+4	No			x
5-5E	1+2	No		x	
5-1W	2+4	Yes			
5-6W <sup>a</sup>	6+5	No <sup>b</sup>	x		
6-11E	1E+1W	-- <sup>b</sup>			
6-6E	1+2	-- <sup>b</sup>			
6-1E	6+5	-- <sup>b</sup>			
6-4W <sup>a</sup>	1+2	-- <sup>b</sup>			
6-7W <sup>a</sup>	3E+3W	-- <sup>b</sup>			
6-7W <sup>a</sup>	3E+4	-- <sup>b</sup>			
7-6E	4E+4W	-- <sup>b</sup>			
7-2W	4+3	No			x
7-3W	1+2	Yes			
7-4W	1+2	No		x	
8-2W	5+6	Yes			
8-5W	2+1	No	x		
9-4E	1+2	No		x	
9-1W	1+2	Yes			
9-3W <sup>a</sup>	6+5	No	x		
10-3E	3+4	No		x	
0-1E	7+8	No			x
10-2W <sup>a</sup>	9+10	No		x	
11-2W	8+7	No	x	—	—
		12	4	5	3

<sup>a</sup>Sites with well control.<sup>b</sup>Not calculated.

difference in time. Only 3 seismic locations within the Manson disturbed area passed all criteria on which the 2-layer dipping refractor model is based.

### Velocity Anisotropy

Of the 46 reverse profile stations which were within the disturbed area, there were 27 stations at which there was no significant difference in the first layer; 12 stations where there was a significant difference in the first layer; and 7 stations where no determination could be made.

At the 12 locations where there was a statistical difference in the first layer, there were 6 locations where there was a significant difference in the second layer and 6 locations where there was not a significant difference. Significant velocity differences in the first layer are explained by the great variability of the unconsolidated drift. Lenticular sand bodies within the drift, variability of both grain size and lithology, and degree of water saturation may have an effect on glacial drift velocities.

At the other 27 stations where the slope test had been made, there were 7 stations where tests of significance in the second layer could not be made and 12 stations where there was not a significant difference in velocity. At the remaining 8 stations, the slope tests for dip calculation were successful. Finally, of these 8 stations, 5 stations did not pass the opposite-intercept test and 3 stations did pass. Only at these 3 sites may a simple 2-layer model with a dipping interface be applied. This is approximately 9% of the total number of stations within the Manson disturbed area. Those stations where significant velocity differences in the second layer were found, indicate that the first bedrock layer was anisotropic to seismic waves.

### Velocity Reversals and Hidden Layers

Before the areal distribution of the first bedrock velocity may be considered, the presence of a layer between the glacial drift and the

bedrock must be considered. If the velocity of this material is lower than the velocity of the glacial drift, the layer will be totally undetected by the horizontal refraction method and will only be revealed by borehole seismic measurements. The effect of a velocity reversal is to reduce the velocity of the upper layer. In other words, an average velocity is obtained for the first 2 layers. Because the first layer for this area of study is glacial drift, the presence of an appreciable number of cases where a second layer with a velocity lower than that of the glacial drift would skew the distribution to the left. From the distributions of the first layer velocity in Figure 7, this is not the case, with the possible exception of one occurrence of a first layer between 1450 and 1500 m/sec.

Green (1962) has investigated the case where a layer has a velocity between the velocity of an overlying layer and the velocity of an underlying layer, but whose thickness is below a certain critical thickness. In such a case the layer will not be detected; therefore both the velocity and the thickness will not be measurable. Hence it is a hidden layer. There are also cases where a refractor is not detected due to the spacing of the geophones. In the former case, the refractor is a true hidden layer because it will never be recorded regardless of the geophone spacing. In the later case, the refractor is an apparent hidden layer.

A true hidden layer between the first and second layer, whose velocity was intermediate between the two, was suspected at six locations (3-3E, 4-1E, 5-1E, 5-4E, 8-6E, and 11-1W)(Figure 1). Unfortunately well logs from boreholes near these sites did not reveal the presence of either a recognizable basal lithologic unit in the glacial drift or an unusual first bedrock unit.



At locations 3-3E, 4-1E, and 8-6E a hidden layer velocity of 2300, 2200, and 2250 m/sec, respectively, was assumed. These were chosen by averaging the second layer velocities from stations east and west of these sites. Calculations based on Green's method were performed on the velocities and intercepts at these sites, and the maximum thickness of a true hidden layer for each record was determined.

At sites 5-1E and 5-4E results from shots in one direction were inconsistent with the rest of the records and were discarded. At site 11-1W no hidden layer velocity was assigned because the velocity of the Pennsylvanian shales and sandstones in the area have not been measured accurately.

#### Velocity Contrast

Once a reasonably accurate representation of the first bedrock layer has been established, the areal distribution of the velocities will reflect, in some fashion, the lateral variations of the bedrock material. These results are presented on the left side of Figure 9. The graphs were computed by averaging the data by refraction line. There appears to be no trend in the averaged first layer (glacial drift) velocities. The averaged glacial drift velocity of 2143 m/sec on line 4 is unexplainably high. The second layer velocity for individual velocities below 3000 m/sec is presented to illustrate the variations in the disturbed shale bedrock. Rather prominent regions of higher velocity are present on line 2 and 9. The utility of the algorithm developed previously is demonstrated on line 4 where there is a lack of velocity contrast between the first and second layer velocities. In such cases the statistical determinations of the best fit line segments may be the only method by which consistent velocity data may be obtained.

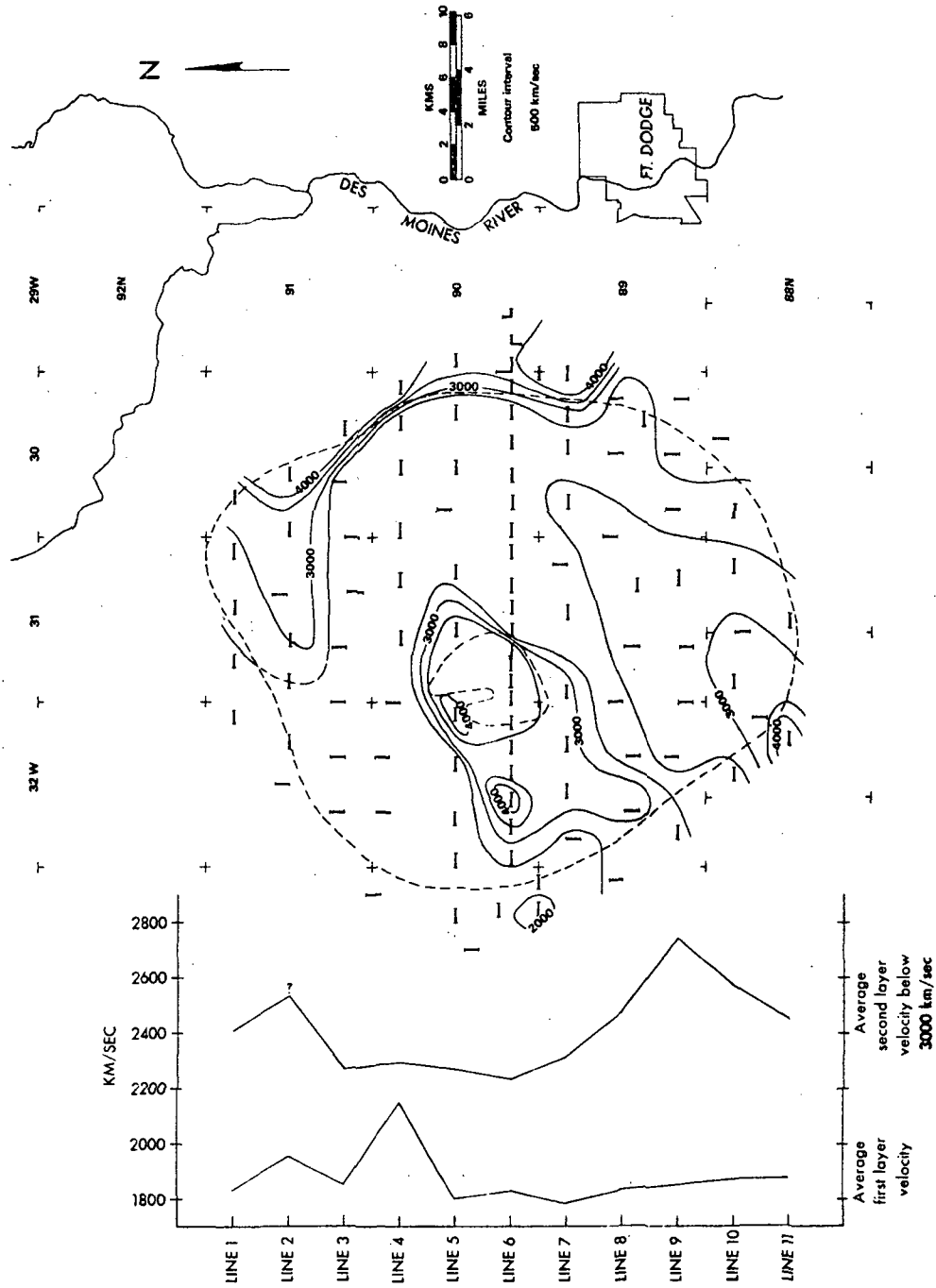


Figure 9. Bedrock velocity graph and contour map of the Manson disturbed area

## BEDROCK VELOCITY AND TOPOGRAPHY

The mean velocity of the two first bedrock velocities, measured at each station, was chosen to approximate the true bedrock velocity. Here, the first line segment is chosen to represent the velocity of glacial drift, and the second line segment is chosen to represent the velocity of the first bedrock layer. This calculation is always higher than the true velocity of the bedrock, if all requirements for dip calculations have been met on the seismic plots. The equation of the true refractor velocity, as presented by Nettleton (1940, p. 269), may be rewritten in terms of mean velocity. Let  $V$  be the true refractor velocity,  $\theta$  be the apparent dip angle, and  $\langle V \rangle$  be the mean velocity of the refractor as measured from opposite directions at a seismic station, then  $V = [4R/(1+R)^2] \cos \theta \langle V \rangle$ , where  $R$  is the ratio of the lower refractor layer velocity to the higher refractor layer velocity. The measurement  $\langle V \rangle$  is less than 5% greater than  $V$  for  $R > 0.68$  and  $\theta < 16^\circ$ . For all stations in the Manson area  $R > 0.65$ . Therefore, the mean velocity of the first bedrock layer is less than 5% higher than the true first bedrock velocity.

The areal distribution of the first bedrock layer is shown on Figure 9. The area in the center of figure bounded by the 3500 m/sec contour roughly coincides with the area of crystalline rock, as determined by borehole methods. Another area of high bedrock velocity is located 10 km due west of the center of the Manson structure and has a diameter of 2 km. It is reasonable to assume that the crystalline rock also subcrops in this area. The limestones and dolomites which comprise the bedrock on the eastern flank of the undisturbed area are delineated quite well by the 4000 m/sec

contour, but velocity data alone may not be used to delineate the edge of the disturbed area elsewhere. Borehole information near location 11-1W reveals that the first bedrock layer, Pennsylvania shales and sandstones, is approximately 3 m thick in this area. The bedrock velocity at station 11-1W reflects the velocity of the underlying Mississippian limestone and sandstones, and the Pennsylvanian shales and sandstones have been averaged in with the glacial drift.

The determination of the depth to the seismic refractors may be calculated by a variety of methods. A method employing the concept of delay time, introduced by Gardner (1939), has been successfully applied [for example the study by Pakiser and Black (1957)]. A similar method employing the concept known as time-depth was developed by Hagedoorn (1959) and Hawkins (1961). Both of these methods make some assumption as to the ray-path. Because the bedrock is suspected of having velocity anisotropy and an irregular surface, depth determinations were made with the velocity-time intercept method, presented by Nettleton (1940), Dobrin (1960), and Steinhart and Meyer (1961). Because very few seismic records could be subjected to dip calculations, depth calculations were based on a simple horizontal model.

In view of the obvious simplicity of this model, error bounds on the depth determinations were made purposefully high. Let the first layer correspond to the first line segment,  $j=1$ . The error bounds of depth to the top of say the  $j$ th layer ( $j>1$ ) were calculated with error bounds on the parameters of the  $j$ th line segment. Confidence limits were chosen so that there was a .99 probability that the true time intercept and wave slowness were within the calculated bounds. The time intercept and wave slowness

for the first to the jth line segment were first used to calculate the depth to the top of the jth layer. The lower depth bound was found by substituting the value of the upper confidence limit of the time intercept and the value of the lower confidence limit of the wave slowness of the jth regression line and then by recalculating the depth. The upper depth bound was found by substituting the value of the lower confidence limit of the time intercept and the value of the upper confidence limit of the wave slowness and then by recalculating the depth. The upper and lower equations for the jth line segment with  $n$  data points are

$$\begin{aligned} t_i^u &= a_j + \tau\sigma_j(a) + [b_j + \tau\sigma_j(b)]d_i \\ t_i^l &= a_j - \tau\sigma_j(a) + [b_j + \tau\sigma_j(b)]d_i \end{aligned} \quad (34)$$

where the superscripts  $u$  and  $l$  indicate the times for the upper and lower line segments and where  $\tau$  is Student's  $\tau_{0.01}$  with  $(n-2)$  degrees of freedom.

Figure 10 is based on an interpretation of a combination of the areal distribution of the depth determinations and bedrock elevations from boreholes. The irregular surface within the Manson disturbed area is sharply contrasted by the gentle slopes outside the area. The average elevation within the boundaries of the disturbed area is about 300 m above sea level, whereas the 320 m contour line roughly traces the average elevation of the undisturbed bedrock surface outside the boundaries. Within the disturbed area a number of bedrock highs and lows are prominent. The central area of crystalline bedrock is seen to be a topographic high. Hills of disturbed shale in the northeast and southwest portion of the disturbed area are present. Six closed depressions surround these bedrock highs. The

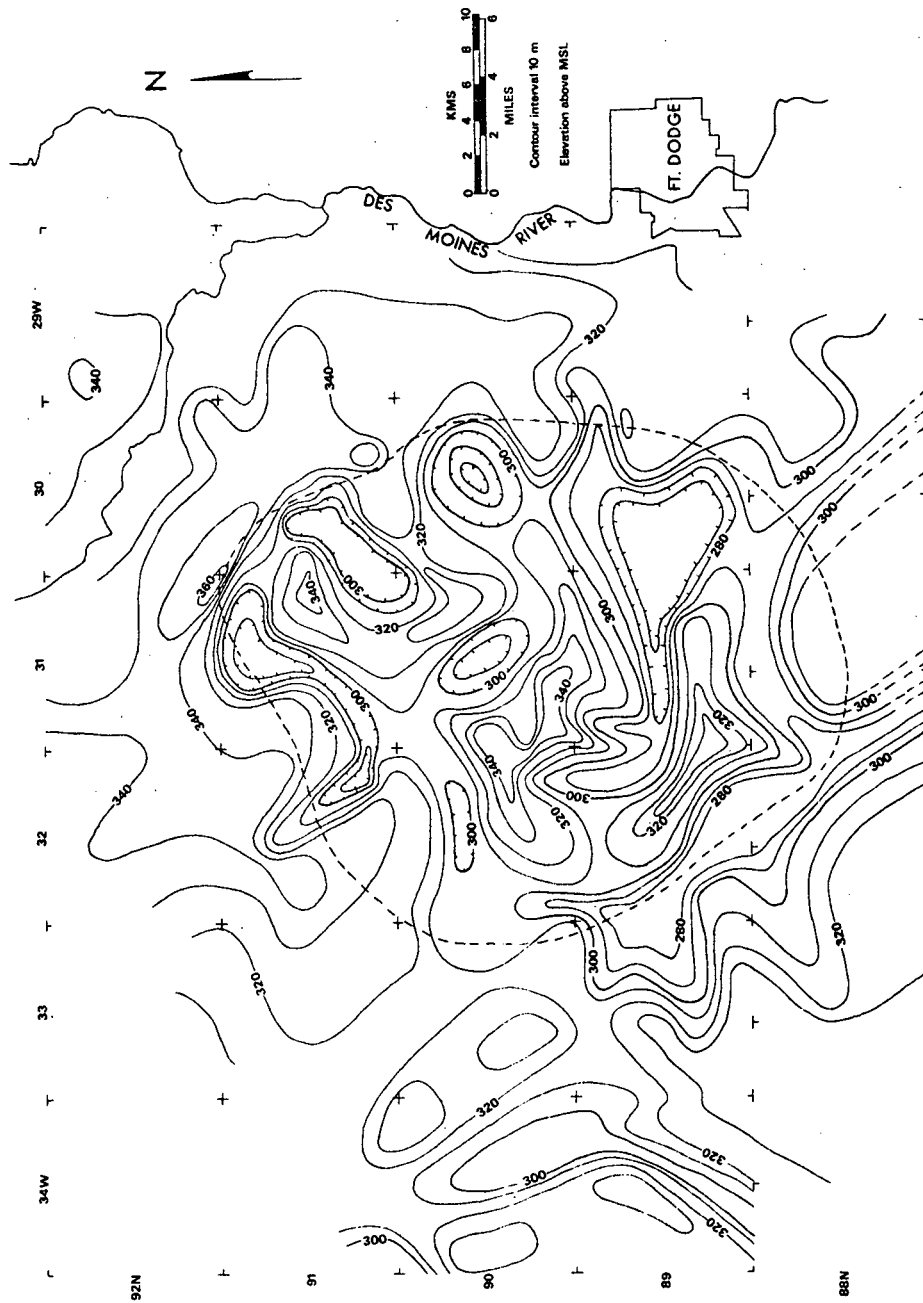


Figure 10. Bedrock topographic contour map of the Manson disturbed area

drainage ways of the disturbed area are not well developed. Several undisturbed bedrock valleys terminate in the depressed area. Two bedrock valleys in the southern portion trend northwest-southeast and their gradient is toward the southeast, away from the disturbed area. The eastern bedrock valley is a headward extension of the bedrock valley shown by Hale (1955, p. 151) to extend southeast across the southwest corner of Webster county. The major drainage network in north-central Iowa is known to drain to the southeast.

## DISCUSSION

A number of features have come to light from the seismic investigation. The Manson disturbed area has been shown to have the appearance of an impact crater. A central uplift of extremely deformed crystalline rock, which was lifted some 700 m from the basement, now extends through a shallow circular basin of highly deformed Cretaceous shales. At the time of burial by Pleistocene drift, the area surrounding the uplift had not developed an integrated drainage network, but occurred as a number of rises and shallow closed depressions. The lack of an integrated drainage network within the disturbed area may indicate that the structure is relatively young.

The relative erosional resistance of the Mississippian limestones and dolomites beyond the northeast rim of the area contrasts with the lack of resistance to erosion of the Pennsylvanian shales and sandstones beyond the southwest rim. This is expressed by the very steep slope along the rim in the northeast and the more gentle slope along the south and southwest rims. Two rather extensive headward erosion channels had developed in the Pennsylvanian shales and sandstones prior to burial. The western bedrock valley follows the edge of the disturbed area for some distance. The zone between the disturbed and undisturbed bedrock must have been less resistant to erosion than either the disturbed or undisturbed bedrock. The shape of the western bedrock valley suggests that the disturbed bedrock was comparatively more erosionally resistant than the undisturbed Pennsylvanian shales.

The second crystalline subcrop, as suggested by the bedrock velocity map, is also seen to be a western extension of the center crystalline



bedrock high. Indeed, the gravity high (Figure 3) in the area coincides with this suspected subcrop of crystalline rock. The elongate 4605 gamma magnetic anomaly (Figure 2) is situated parallel to the crystalline bedrock high and shifted 1 km to the east.

Only 20% of the seismic records taken at sites well within the Manson disturbed area could be represented by a 3-layer seismic model. At many of these sites the third layer detected by a shot in one direction was not detected in the shot record in the other direction. A third layer with velocity about 3400 m/sec may be present below sites 3-2E and 3-1E, but the depths to this layer are quite irregular and dip calculations could not be made. For the most part, there is no mappable seismic refractor, below that of the drift-shale interface, to a depth of 250 m.

The rim structure appears to have considerable complexity. The line segments fitted to the records at stations 6-13E to 6-16E showed that there is a large variation of velocity in the undisturbed bedrock east of the Manson disturbed area (seen earlier). No consistent structural model, no matter how general, could be made of the geometric arrangement of the bedrock layers. Simple seismic models may not be applied in these areas, and it points to considerable geologic complexity, probably due to complex folding of the bedrock units adjacent to the Manson disturbed area.

Another significant feature is the seismic velocity of the crystalline rock in the center and western portion of the structure. Press (1966) has reported that granite velocities may range from 4.8 to 5.9 m/sec. Velocity histograms of granite and gneiss were presented by Hasselstrom (1969) for shallow seismic refraction measurements. In each case at least 75% of the sample had a velocity greater than 5000 m/sec. At Manson the velocity of

the mixture of granite, gneiss, and diabase is between 3000 and 5000 m/sec and averages near 4000 m/sec. The unusually low velocity of this crystalline mass may indicate that this rock body has an abnormally high porosity. This may be a result of the large scale brecciation of the crystalline mass during the emplacement event.

The unusual deformation characteristics of the minerals of the central crystalline mass have shown that this structure could have been created by one of only two 'catastrophic' events. Several similarities of the Manson structure to the Canadian craters are noted. This crystalline rock has a close similarity to rocks taken from central uplifts in larger Canadian craters, and the age of this crystalline mass is near the approximate age of the basement rock as observed in some Canadian craters (Michael Dence, personal communication, 1970).

Regardless of which mechanism had created the structure, the basement rock would be involved in the final disposition of the materials, because the thickness of the sedimentary column is considerably less than the diameter of the structure (roughly 1:400). Therefore gravity and magnetic anomalies from the upthrown basement rock may not be used to distinguish between the two mechanisms.

The questions raised by the occurrence of this complex structure must be answered by sifting and evaluating a wealth of data, some of which is contradictory or coincidental. The nature of the origin of the Manson disturbed area must await the collection and interpretation of additional data.

## LITERATURE CITED

- Bellman, Richard and Robert Roth. 1969. Curve fitting by segmented straight lines. American Statistical Association Journal 64: 1079-1084.
- Bevington, Philip R. 1969. Data reduction and error analysis for the physical sciences. New York, New York, McGraw-Hill Book Company, Inc.
- Borcherdt, R. D. and J. H. Healy. 1968. A method for estimating the uncertainty of seismic velocities measured by refraction techniques. Seismological Society of America Bulletin 58: 1769-1790.
- Bucher, Walter H. 1936. Cryptovolcanic structures in the United States. International Geological Congress, 16th, United States 1933, Reports 2: 1055-1084.
- Bunch, T. E. 1968. Some characteristics of selected minerals from craters. In French, B. M. and N. M. Short, editors. Shock Metamorphism of Natural Materials. Pp. 413-432. Baltimore, Maryland, Mono Book Inc.
- Coons, Richard L., George P. Woollard, and Garland Hershey. 1967. Structural significance and analysis of mid-continent gravity high. American Association of Petroleum Geologists Bulletin 51: 2381-2399.
- Dobrin, Milton B. 1960. Introduction to geophysical prospecting. 2nd edition. New York, New York, McGraw-Hill Book Co., Inc.
- Dryden, J. E. 1955. A study of a well core from crystalline rocks near Manson, Iowa. Unpublished Master's thesis. Iowa City, Iowa, Library, University of Iowa.
- Gardner, L. W. 1939. An areal plan of mapping subsurface structure by refraction shooting. Geophysics 4: 247-259.
- Green, R. 1962. The hidden layer problem. Geophysical Prospecting 10: 166-170.
- Hagedoorn, J. G. 1959. The plus-minus method of interpreting seismic refraction sections. Geophysical Prospecting 7: 158-182.
- Hale, William E. 1955. Geology and ground-water resources of Webster County, Iowa. Des Moines, Iowa, State of Iowa.
- Hasselstrom, B. 1969. Applications of the seismic refraction method. Geoexploration 7: 113-132.
- Hawkins, L. V. 1961. The reciprocal method of routine seismic investigations. Geophysics 26: 806-819.

- Henderson, J. R., W. S. White, and J. Zietz. 1963. Preliminary interpretation of an aeromagnetic survey in north-central Iowa. Washington, D.C., United States Geological Survey, Open File Report.
- Henderson, J. R. and Joseph L. Vargo. 1965. Aeromagnetic map of central Iowa. Washington, D.C., United States Geological Survey, Geophysical Investigations Map GP-476.
- Hobson, George D. 1969. Seismic methods in mining and groundwater exploration. In Morley, L. W., editor. Mining and groundwater geophysics/1967. Pp. 148-176. Ottawa, Canada, Queen's Printer of Canada.
- Holtzman, Allan F. 1970. Gravity study of the Manson disturbed area, Calhoun, Pocahontas, Humboldt, and Webster Counties, Iowa. Unpublished Master's thesis. Iowa City, Iowa, Library, University of Iowa.
- Hoppin, R. A. and J. E. Dryden. 1958. An unusual occurrence of pre-Cambrian crystalline rocks beneath glacial drift near Manson, Iowa. *Journal of Geology* 66: 694-699.
- Hudson, Derek J. 1966. Fitting segmented curves whose join points have to be estimated. *American Statistical Association Journal* 61: 1097-1129.
- Iowa Geological Survey. 1969. Geologic Map of Iowa. Iowa City, Iowa, Iowa Geological Survey.
- Iyer, H. M., L. C. Pakiser, D. J. Stuart, and D. H. Warren. 1969. Project Early Rise: seismic probing of the upper mantle. *Journal of Geophysical Research* 74: 4409-4441.
- Kaila, K. L. and Hari Narain. 1970. Interpretation of seismic refraction data and the solution of the hidden layer problem. *Geophysics* 35: 613-623.
- Lennox, D. H. and V. Carlson. 1969. Integration of geophysical methods for groundwater exploration in the prairie provinces, Canada. In Morley, L. W., editor. Mining and groundwater geophysics/1967. Pp. 517-533. Ottawa, Canada, Queen's Printer of Canada.
- Lidiak, Edward G., Richard F. Marvin, Herman H. Thomas, and Manuel N. Bass. 1966. Geochronology of the mid-continent region, United States. *Journal of Geophysical Research* 71: 5427-5438.
- McGee, Victor E. and Willard T. Carleton. 1970. Piecewise regression. *American Statistical Association Journal* 65: 1109-1124.
- Nettleton, L. L. 1940. Geophysical prospecting for oil. New York, New York, McGraw-Hill Book Company, Inc.

- Pakiser, L. C. and R. A. Black. 1957. Exploring for ancient channels with the refraction seismograph. *Geophysics* 22: 32-47.
- Press, Frank. 1966. Seismic velocities. In Clark, S. P., Jr., editor. *Handbook of Physical Constants*. New York Geological Society of America Memoir 97: 197-198.
- Quandt, Richard E. 1958a. Tests of the hypothesis that a linear regression system obeys two separate regimes. *American Statistical Association Journal* 53: 324-330.
- Quandt, Richard E. 1958b. The estimation of the parameters of a linear system obeying two separate regimes. *American Statistical Association Journal* 53: 873-880.
- Robinson, D. E. 1964. Estimates for the point of intersection of two polynomial regressions. *American Statistical Association Journal* 59: 214-224.
- Sprent, P. 1961. Some hypotheses concerning two phase regression lines. *Biometrics* 17: 634-645.
- Staub, William P. 1969. Seismic refraction, a technique for subsurface investigation in Iowa. Unpublished Ph.D. thesis. Ames, Iowa, Library, Iowa State University of Science and Technology.
- Steinhart, John S. and Robert P. Meyer. 1961. Minimum statistical uncertainty of the seismic refraction profile. *Geophysics* 26: 574-587.
- Wampler, Roy H. 1970. A report on the accuracy of some widely used least squares computer programs. *American Statistical Association Journal* 65: 549-565.
- Wine, R. Lowell. 1964. *Statistics for scientists and engineers*. Edge-wood Cliffs, New Jersey, Prentice-Hall, Inc.
- Yoho, W. Herbert. 1967. Preliminary report on basement complex rocks of Iowa. Iowa City, Iowa, Iowa Geological Survey Report of Investigations 3.

## ACKNOWLEDGEMENTS

We wish to thank the many people who assisted in the collection of field data and in particular to Don Neading and Marv Taylor for their efforts in securing high quality measurements and efficient field operations. And for many stimulating discussions on the application of statistics to geologic problems and for suggesting the application of analysis of covariance to several regression lines we wish to thank Randy Stone of the Department of Earth Science. For their support of the major portion of this research, we thank the National Aeronautics and Space Administration and Jack Hartung of the Houston Manned Space-flight Center for his interest.

## APPENDIX A. LIST OF THE COMPUTER PROGRAM

1. Purpose:

The program fits joined regression lines to an ordered series of measurements on the basis of residual sum of squares. For each line segment, the parameters and their standard deviations are calculated. The measurements are taken to be seismic refraction time-distance pairs, and from the results of the line fitting analysis, depths and depth error bounds are determined.

2. Method:

The set of up to 24 time-distance measurements are sequentially partitioned into subsets of data, each of which is searched for the best 2 segment fit. Each subset has an upper bound, which is chosen prior to the analysis, and a lower bound, which is determined by the position of the join point from a preceding 2 segment fit. The final solution is derived from a combination of the 2 segment fits.

For a subset of data, pairs of regression lines are fitted to all combinations of the data, and the pair of regression lines which have the least combined residual sum of squares are taken to be the best fit.

Least squares regression is used to best fit the line segments. The intercept and wave slowness (parameters  $a$  and  $b$ ) of each regression line are calculated, and under the assumption that the variable, time, is independently and normally distributed with constant variance, the standard deviations of intercept and wave slowness are found. The depth calculations are based on the standard time intercept-wave slowness equations. Error bounds in depth have been treated previously.

### 3. Accuracy:

The accuracy of the program was measured from test data presented in Table 3. These data were analyzed by (1) the OMNITAB program available at the Iowa State Computation Center, (2) a least squares program written by Bevington (1969), and (3) a subroutine from this program, SJOIN. All programs were run on the Computation Center's IBM 360/65. An evaluation of widely used regression programs by Wampler (1970) found that the single precision OMNITAB program is correct to 4 and 6 significant figures for the first two coefficients of a fifth degree polynomial. From the test data, the calculations of a and b by subroutine SJOIN agree with those from the OMNITAB program to 5 and 6 figures (Table 4). The standard deviations of a and b agree to 7 and 6 figures. The calculations of residual sum of squares from the subroutine SJOIN and program OMNITAB are included. The results of the Bevington program are presented as another comparison.

Because the calculation of residual sum of squares is fundamental to the validity of the program, the time values,  $t$  (Table 3), were adjusted for a range of values. The results are presented in Table 5. The approximate range of values used in the analysis of the data from this study were  $0 < d < 800$  and  $0.005 < t < 0.450$ , so the residual sum of squares calculations are valid to approximately 5 significant figures. Because any 2 calculations of the residual sum of squares were equal to at most 4 digits, the program is considered to be valid for the statistical decisions undertaken.



Table 3. Test data of distance, d, and time, t

d	t
15.	12.
90.	28.
195.	45.
300.	63.
405.	82.

Table 4. Comparison of three computer programs

Coefficient	Program		
	SJOIN <sup>a</sup>	OMNITAB <sup>b</sup>	Bevington <sup>a</sup>
a <sup>c</sup>	10.53826	10.538361	10.538420
$\sigma(a)$	0.91706004	0.91706008	0.916853
b	0.17642574	0.17642599	0.176426
$\sigma(b) \times 10^{-2}$	0.37415442	0.37415458	0.3741
RSS <sup>d</sup>	4.1312900	4.1345215	--

<sup>a</sup>Double precision.

<sup>b</sup>Single precision.

<sup>c</sup>The form of the equation is  $t = a + bd$ .

<sup>d</sup>Residual sum of squares.

Table 5. Significant figures of the calculation of residual sum of squares for various values of time

Data	Approximate velocity <sup>a</sup>	Significant figures <sup>b</sup>
$(d_i, t_i)^c$	5.833	$\geq 13$
$(d_i, 0.1t_i)$	58.33	5
$(d_i, 0.01t_i)$	583.3	6
$(d_i, 0.001t_i)$	5833.	4

<sup>a</sup>Velocity is the reciprocal of b.

<sup>b</sup>Based on the manual calculation  $RSS = 4.131290027447$ .

<sup>c</sup>Where  $i = 1, \dots, 5$ .

#### 4. Usage:

##### a. Input:

A standardized punched card record format is described in the comment cards of subroutine RREC.

##### b. Output:

Although the length of the output is a function of the number of fitted line segments, the number of data, and the number of acceptable regression candidates, a typical 2 segment analysis of 24 data points will yield about 1 page of printed output.

##### c. Operating Procedures:

The first card of the data deck must specify the mode of operation

of the program (see the comments in the main program). The next 2 cards must be the first 24 Student's values with a format of D6.3. The input records then follow. The end of data is specified by placing a blank card and a card with 99 punched in cols. 47-48 after the final record.

d. Constants:

A total of 4560 bytes has been allocated to unlabeled COMMON and 116 bytes to COMMON area /LABEL/.

5. Subroutines Required:

The subroutines required are RREC, SETS, SJOIN, CJOIN, OUTPUT, and ABYSS. The main program calls subroutines RREC, SETS, and ABYSS. Subroutines SETS calls subroutines SJOIN, CJOIN, and OUTPUT.

A list of the program follows.

```

C
C
C
C
C
001
002
003
004
005
006
007
008
009
010
011
012
013
014
015
016
017
018
019
020
021
022
023
024
025
026
027
028
029
030
031
032
033
034
035
036
037

      SET UP TO APPLY SETS AND ABYSS TO REDUCED RECORDS

      SUBROUTINES REQUIRED:  RREC,SETS,ABYSS

      REAL*8 BETA(12,23),STD(8,23),GAMMA(5,22),DELTA(6,6),AMIN
      REAL*8 ZETA(6,5),S(24)
      INTEGER*4 NREAD/1/,NPUNCH/2/,NPRINT/3/
      INTEGER*4 ID(5)
      REAL T(49),D(49)
      INTEGER IU(10),II(24),NPTS(6)
      COMMON BETA,STD,GAMMA
      COMMON/LABEL/ID,II

      THE FIRST CARD PROVIDES THE USER WITH SEVERAL PROGRAMMING OPTIONS.
      COL. 1 = 0 DATA ANALYZED AS PER TEST POINT VECTOR.
            = 1 DATA ANALYZED AS PER TEST POINT VECTOR AND 2-LAYER MODEL.
            = 2 DATA ANALYZED AS 2-LAYER MODEL ONLY.
      COL. 2 = 0 VELOCITY CARDS NOT PUNCHED.
            = 1 VELOCITY CARDS PUNCHED.
      COL. 3 = 0 DEPTH DETERMINATIONS ARE NOT CALCULATED.
            = 1 DEPTH DETERMINATIONS ARE CALCULATED.

      READ (NREAD,8) KK,KL,KM
      8 FORMAT (3I1)

      THE SECOND AND THIRD CARDS ARE THE STUDENT'S T CONSTANTS.

      READ(NREAD,9) (S(I),I = 1,24)
      9 FORMAT (12D6.3)

      DO 10 I = 1,24
      10 II(I) = I
      1 CALL RREC (L,LL,IEND,T,D,10,IU)
      IF (L.EQ.99) GO TO 99
      KA = 0
      DO 20 ITEST = 1,10

```

```

038 IF (IU(ITEST).EQ.0) GO TO 3
039 20 CONTINUE
040 ITEST = 11
041 3 KA = KA + 1
042 IF (KK.EQ.2) ITEST = 1
043 AMIN = 0.00
044 WRITE (NPRINT,5)
045 5 FORMAT ('1')
046 CALL SETS (IEND,ITEST,IU,T,D,IDEL,DELTA,NPTS,AMIN)
047 WRITE (NPRINT,29)
048 29 FORMAT ('0',132('#')) /' LAYER',4X,'INTERCEPT',4X,'STD OF INT',7X,
049 X 'SLOPE',7X,'STD OF S',4X,'VELOCITY',4X,'RESID SS',6X,'N PTS' /
050 X ' ',132('#'))
051 DO 30 I = 1,IDEL
052 30 WRITE (NPRINT,31) I,(DELTA(J,I),J = 1,6),NPTS(I)
053 31 FORMAT (' ',3X,12,3X,F10.4,3(2X,D12.5),5X,F5.0,2X,D12.5,7X,12)
054 WRITE (NPRINT,32) AMIN
055 32 FORMAT ('0TOTAL RESIDUAL SUM OF SQUARES = ',D20.8)
056
057 PUNCH UP LAYER DATA
058
059 IF (KL.EQ.0) GO TO 33
060 WRITE (NPUNCH,50) ID,IDEL
061 50 FORMAT (5A4,2X,12)
062 DO 60 I = 1,IDEL
063 60 WRITE (NPUNCH,61) NPTS(I),(DELTA(J,I),J = 1,6)
064 61 FORMAT (4X,12,2X,6D12.5)
065
066 FIND DEPTHS BOTH WITH AND WITHOUT THE LVL
067
068 33 IF ((IDEL.EQ.1).OR.(KM.EQ.0)) GO TO 70
069 WRITE (NPRINT,34)
070 34 FORMAT ('1',/3('#-')/' ' ,132('#='))
071 KKK = 0
072 35 KKK = KKK + 1
073 CALL ABYSS (IDEL,NPTS,S,DELTA,ZETA)
074 IF (KKK.EQ.2) WRITE (NPRINT,36)

```

C  
C  
C

C  
C  
C

```

075 36 FORMAT (' WITH LOW VELOCITY LAYER')
076 WRITE (NPRINT,37) ID,IDEL
077 37 FORMAT ('0',10X,'RECORD ',5A4,' NUMBER OF LAYERS ',I2/'ON PTS',
078 X 4X,'INTERCEPT',3X,'STD OF INT',4X,'SLOPE',5X,'STD OF S',4X,
079 X 'VELOCITY',4X,'RESID MS')
080 DO 6 I = 1,IDEL
081 6 WRITE (NPRINT,38) NPTS(I),(DELTA(J,I),J = 1,6)
082 38 FORMAT (4X,I2,2X,6D12.5)
083 WRITE (NPRINT,39)
084 39 FORMAT ('0',9X,'THICKNESS',2X,'UPPER LIMIT',2X,'LOWER LIMIT',4X,
085 X 'DEPTH',4X,'LOWER LIMIT',2X,'UPPER LIMIT')
086 IF = IDEL - 1
087 DO 40 I = 1,IF
088 40 WRITE (NPRINT,41) (ZETA(J,I),J = 1,6)
089 41 FORMAT (11X,F7.2,5X,F7.2,6X,F7.2,4X,F7.2,5X,F7.2,6X,F7.2,
090 X 10X,'IN METERS')
091 WRITE (NPRINT,39)
092 DO 43 J = 1,IF
093 DO 42 I = 1,6
094 42 ZETA(I,J) = ZETA(I,J) * 3.2803D0
095 43 WRITE (NPRINT,44) (ZETA(I,J),I = 1,6)
096 44 FORMAT (11X,F7.2,5X,F7.2,6X,F7.2,4X,F7.2,5X,F7.2,6X,F7.2,
097 X 10X,'IN FEET')
098 WRITE (NPRINT,45)
099 45 FORMAT ('0',132('='))
100 IF (KKK.EQ.2) GO TO 70
101
102 SET FIRST LAYER TO HAVE AIR-WAVE CHARACTERISTICS
103
104 IA = IDEL + 1
105 IB = IDEL + 2
106 DO 46 I = 1,IDEL
107 NPTS(IB - I) = NPTS(IA - I)
108 DO 46 J = 1,6
109 46 DELTA(J,IB - I) = DELTA(J,IA - I)
110 IDEL = IDEL + 1
111 NPTS(1) = 0

```

C  
C  
C

112  
113  
114  
115  
116  
117  
118  
119  
120  
121  
122  
123  
124  
125  
126  
127

```

DELTA(1,1) = 0.00
DELTA(2,1) = 0.00
DELTA(3,1) = 3.01705D-03
DELTA(4,1) = 0.00
DELTA(5,1) = 0.00
DELTA(6,1) = 0.00
GO TO 35

C
70 IF (ITEST.EQ.1) GO TO 75
   ITEST = 1
   IF ((KK.EQ.1).AND.(KA.EQ.1)) GO TO 3
75 GO TO 1
99 IF (KL.EQ.1) WRITE (NPRINT,100)
100 FORMAT ('--',10X,'VELOCITY CARDS HAVE BEEN PUNCHED')
    STOP
    END

```

SUBROUTINE RREC (L,LL,IEND,T,D,LIU,IU) RREC001

```

*****
*
* SUBROUTINE RREC READS REDUCED SEISMIC RECORDS. THE COMMAND CARD PREFAC-
* ING EACH RECORD IS READ FOR UP TO 10 TEST POINTS AS WELL.
* ARGUMENTS
* L = END OF DATA SET CODE. WHEN 99 IS READ, IT SIGNALS
* L = THE END OF THE DATA SET.
* LL = SPREAD GEOMETRY CODE
* IEND = LENGTH OF T AND D
* T = TIME VECTOR
* D = DISTANCE VECTOR
* LIU = LENGTH OF TEST POINT VECTOR
* IU = TEST POINT VECTOR
*
* REDUCED RECORD FORMAT REMARK
* CARD COLUMN
*
*-----*
* COMMAND CARD
* 1-2 M = BATCHING CODE
* 3-4 ISEL = SELECTION CODE
* -----
* 6-7 PAIRS OF VALUES FOR TEST POINT VECTOR.
* -----
* CONTINUES TO COLUMN 25 TOTAL OF 10 VALUES.
*
*-----*
* IDENTIFICATION CARD
* 1-20 IDENTIFICATION
* 21-22 SPREAD GEOMETRY CODE
* 47-48 END OF DATA SET FIELD
*
*-----*
* TIME CARDS
* 1-5 LENGTH OF TIME VECTOR
*
*****

```







```

C
INTEGER IU(10), INDEX(22), NPTS(1)
COMMON BETA, STD, GAMMA
IDEL = 0
ISHIFT = 0
ISAVE = 0
MARK = -1
IU(ITEST) = IEND
IM = 0
I1 = 1
I2 = 1

DO 50 I = 1, ITEST
  L = IU(I) - ISHIFT
  IF (L.LT.4) GO TO 50
  K = 0
  DO 8 J = 1, L
    ST(J) = T(J + ISHIFT)
    8 SD(J) = D(J + ISHIFT)
    IS = ISHIFT
    9 CALL SJOIN (L, ST, SD)
    CALL CJOIN (L, O, SD, INDEX, TMIN, ITMIN, SMIN, ISMIN)
    CALL OUTPUT (L, ST, SD, INDEX, I, IS)
    WRITE (NPRINT, 1) ITMIN, TMIN, ISMIN, SMIN
    1 FORMAT (' T INDEX=', I3, ' MINIMUM T=', D13.5, I0X, ' S INDEX=', I3,
      X ' MINIMUM S=', D13.5)
    IF ((TMIN.EQ.1.D70).AND.(SMIN.EQ.1.D70)) GO TO 50
    IF (TMIN.EQ.1.D70) GO TO 20
    IF (SMIN.EQ.1.D70) GO TO 10
    IF (TMIN.GT.SMIN) GO TO 20
    T CANDIDATE
    10 ISHIFT = ITMIN + 1 + ISHIFT
    IF (.NOT.(((MARK + 1).EQ.1).AND.(K.EQ.0))) GO TO 12
    NPTS(IDEL + 3) = L - ITMIN - 1
    DELTA(1, IDEL + 3) = BETA(4, ITMIN)
    DELTA(2, IDEL + 3) = STD(5, ITMIN)
    DELTA(3, IDEL + 3) = BETA(5, ITMIN)
    DELTA(4, IDEL + 3) = STD(6, ITMIN)
  SETS006
  SETS007
  SETS008
  SETS009
  SETS010
  SETS011
  SETS012
  SETS013
  SETS014
  SETS015
  SETS016
  SETS017
  SETS018
  SETS019
  SETS020
  SETS021
  SETS022
  SETS023
  SETS024
  SETS025
  SETS026
  SETS027
  SETS028
  SETS029
  SETS030
  SETS031
  SETS032
  SETS033
  SETS034
  SETS035
  SETS036
  SETS037
  SETS038
  SETS039
  SETS040
  SETS041
  SETS042

```

```

DELTA(5, IDEL + 3) = STD(8, ITMIN)
DELTA(6, IDEL + 3) = BETA(6, ITMIN)
L = ISHIFT - ISAVE
K = K + 1
IS = ISAVE
DO 11 J = 1, L
  ST(J) = T(J + ISAVE)
11 SD(J) = D(J + ISAVE)
  GO TO 9
12 IF ((K.EQ.1).AND.((BETA(5, ITMIN).GT.BETA(2, ITMIN)).OR.
  X (DELTA(3, IDEL + 3).GT.BETA(5, ITMIN)))) GO TO 18
  IF (IDEL.EQ.0) GO TO 13
  IF (DELTA(3, IDEL).LT.BETA(11 + 1, ITMIN)) GO TO 50
13 IDEL = IDEL + 1
  NPTS(IDEL) = ITMIN + 1
  IF (IM.EQ.1) NPTS(IDEL) = L - ITMIN - 1
  DELTA(1, IDEL) = BETA(11, ITMIN)
  DELTA(2, IDEL) = STD(12, ITMIN)
  DELTA(3, IDEL) = BETA(11 + 1, ITMIN)
  DELTA(4, IDEL) = STD(12 + 1, ITMIN)
  DELTA(5, IDEL) = STD(12 + 3, ITMIN)
  DELTA(6, IDEL) = BETA(11 + 2, ITMIN)
  IF (K.EQ.1) GO TO 14
  IF (1.LT.ITEST) GO TO 50
14 IM = IM + 1
  11 = 4
  12 = 5
  GO TO (13), IM
  IM = 0
  IF (K.EQ.1) IDEL = IDEL + 1
  GO TO 50
C
  S CANDIDATE
20 IF ((MARK + 1).NE.1) GO TO 31
  IF ((K.EQ.1).AND.((GAMMA(4, ISMIN).GT.GAMMA(2, ISMIN)).OR.
  X (DELTA(3, IDEL + 3).GT.GAMMA(4, ISMIN)))) GO TO 18
  IF (K.EQ.1) GO TO 23
  IDEL = IDEL + 1

```

SETS043  
 SETS044  
 SETS045  
 SETS046  
 SETS047  
 SETS048  
 SETS049  
 SETS050  
 SETS051  
 SETS052  
 SETS053  
 SETS054  
 SETS055  
 SETS056  
 SETS057  
 SETS058  
 SETS059  
 SETS060  
 SETS061  
 SETS062  
 SETS063  
 SETS064  
 SETS065  
 SETS066  
 SETS067  
 SETS068  
 SETS069  
 SETS070  
 SETS071  
 SETS072  
 SETS073  
 SETS074  
 SETS075  
 SETS076  
 SETS077  
 SETS078  
 SETS079

```

NPTS(IDEL) = ISE
DO 30 J = 1,6
30 DELTA(J,IDEL) = SAVE(J)
31 IF (1.EQ.ITEST) GO TO 21
MARK = I
ISAVE = ISHIFT
ISHIFT = ISMIN + ISHIFT
ISE = ISMIN + 1
SAVE(1) = GAMMA(1,ISMIN)
SAVE(2) = STD(1,ISMIN)
SAVE(3) = GAMMA(2,ISMIN)
SAVE(4) = STD(2,ISMIN)
SAVE(5) = 1.DO / GAMMA(2,ISMIN)
SAVE(6) = BETA(3,ISMIN)
GO TO 50
18 NPTS(IDEL + 3) = 0
DO 19 J = 1,6
19 DELTA(J,IDEL + 3) = 0.DO
GO TO 50
21 IF (GAMMA(4,ISMIN).GT.GAMMA(2,ISMIN)) GO TO 50
IF (IDEL.EQ.0) GO TO 23
IF (GAMMA(2,ISMIN).GT.DELTA(3,IDEL)) GO TO 50
23 KK = 0
I1 = 1
I2 = 1
22 IDEL = IDEL + 1
NPTS(IDEL) = ISMIN + 1
IF (KK.EQ.1) NPTS(IDEL) = L - ISMIN
NOTE: THE STANDARD DEVIATIONS OF THE S CANDIDATE COEFFICIENTS ARE
TAKEN FROM STD AND ARE APPROXIMATIONS OF THE TRUE STANDARD
DEVIATIONS.
DELTA(1,IDEL) = GAMMA(I1,ISMIN)
DELTA(2,IDEL) = STD(I2,ISMIN)
DELTA(3,IDEL) = GAMMA(I1 + 1,ISMIN)
DELTA(4,IDEL) = STD(I2 + 1,ISMIN)
DELTA(5,IDEL) = 1.DO / GAMMA(I1 + 1,ISMIN)
KK = KK + 1

```

SETS080  
 SETS081  
 SETS082  
 SETS083  
 SETS084  
 SETS085  
 SETS086  
 SETS087  
 SETS088  
 SETS089  
 SETS090  
 SETS091  
 SETS092  
 SETS093  
 SETS094  
 SETS095  
 SETS096  
 SETS097  
 SETS098  
 SETS099  
 SETS100  
 SETS101  
 SETS102  
 SETS103  
 SETS104  
 SETS105  
 SETS106  
 SETS107  
 SETS108  
 SETS109  
 SETS110  
 SETS111  
 SETS112  
 SETS113  
 SETS114  
 SETS115  
 SETS116

C  
 C  
 C

```

11 = 3
12 = 5
GO TO (22),KK
DELTA(6,IDEL - 1) = 0.00
DELTA(6,IDEL) = GAMMA(5,ISMIN)
IF (K.EQ.1) IDEL = IDEL + 1
50 CONTINUE
C
IF (IDEL.EQ.0) GO TO 80
AMIN = 0.00
DO 75 I = 1, IDEL
75 AMIN = AMIN + DELTA(6,I)
RETURN
C
IF NO CANDIDATE HAS BEEN FOUND, RUN THE COMPLETE SET.
80 CALL SJOIN (IEND,T,D)
CALL CJOIN (IEND,O,D,INDEX,TMIN,ITMIN,SMIN,ISMIN)
CALL OUTPUT (IEND,T,D,INDEX,O,0)
IDEL = 1
NPTS(1) = IEND
AMIN = BETA(8,IEND - 1)
DELTA(1,1) = BETA(1,IEND - 1)
DELTA(2,1) = STD(1,IEND - 1)
DELTA(3,1) = BETA(2,IEND - 1)
DELTA(4,1) = STD(2,IEND - 1)
DELTA(5,1) = STD(4,IEND - 1)
DELTA(6,1) = BETA(8,IEND - 1)
RETURN
C
DELTA CONSTRAINTS
1. L MUST BE GREATER THAN 3.
2. IF MINIMUM T = MINIMUM S, THE MINIMUM T IS CHOSEN.
3. VELOCITIES MUST MONOTONICALLY INCREASE.
C
C
C
C
C
C
END

```

SETS117  
 SETS118  
 SETS119  
 SETS120  
 SETS121  
 SETS122  
 SETS123  
 SETS124  
 SETS125  
 SETS126  
 SETS127  
 SETS128  
 SETS129  
 SETS130  
 SETS131  
 SETS132  
 SETS133  
 SETS134  
 SETS135  
 SETS136  
 SETS137  
 SETS138  
 SETS139  
 SETS140  
 SETS141  
 SETS142  
 SETS143  
 SETS144  
 SETS145  
 SETS146  
 SETS147  
 SETS148  
 SETS149  
 SETS150

SJOIN001

SUBROUTINE SJOIN (N,Y,X)

```

C *****
C *
C * SUBROUTINE SJOIN CALCULATES A SERIES OF COMBINATIONS OF BEST FIT
C * ESTIMATES OF Y UPON X, WHICH ARE BASED ON A SIMPLE LINEAR MODEL
C *
C *  $Y = A1 + B1 X$  FOR  $X(1) < X < X(N)$ 
C *  $Y = A2 + B2 X$  FOR  $X(I+1) < X < X(N)$ 
C *
C * THE SERIES COMPRISES THOSE COMBINATIONS OF LINES FROM  $I = 2$  TO  $I = N - 2$ 
C * AND A SIMPLE LINEAR MODEL  $Y = A1 + B1 X$  FOR ALL X.
C *
C * N = LENGTH OF X AND Y
C * Y = DEPENDENT VARIABLE VECTOR
C * X = INDEPENDENT VARIABLE VECTOR
C *
C * BETA MUST BE DIMENSIONED 12 X (N-1)
C * STD MUST BE DIMENSIONED 8 X (N-1)
C *
C * THE OUTPUT DATA ARE STORED AS:
C * BETA(1,1)=A1, BETA(2,1)=B1, BETA(3,1)= RESID SUM OF SQUARES
C * BETA(4,1)=A2, BETA(5,1)=B2, BETA(6,1)= RESID SUM OF SQUARES
C * BETA(7,1) = X VALUE OF THE INTERSECTION OF THE TWO LINES
C * BETA(8,1) = COMBINED RESIDUAL SUM OF SQUARES
C * STD(1,1) = STANDARD DEVIATION OF A1
C * STD(2,1) = STANDARD DEVIATION OF B1
C * STD(3,1) = CORRELATION COEFFICIENT
C * STD(4,1) = RECIPROCAL OF B1
C * STD(5,1) = STANDARD DEVIATION OF A2
C * STD(6,1) = STANDARD DEVIATION OF B2
C * STD(7,1) = CORRELATION COEFFICIENT
C * STD(8,1) = RECIPROCAL OF B2
C *
C *****
C *
C IMPLICIT REAL*8 (A-H,O-Z)
C REAL*8 NUM,NUMBER
C REAL X(1),Y(1)
C COMMON BETA(12,23),STD(8,23),GAMMA(5,22)
C JJ = N - 1
C *****

```

SJOIN002

SJOIN003

SJOIN004

SJOIN005

SJOIN006

SJOIN007  
SJOIN008  
SJOIN009  
SJOIN010  
SJOIN011  
SJOIN012  
SJOIN013  
SJOIN014  
SJOIN015  
SJOIN016  
SJOIN017  
SJOIN018  
SJOIN019  
SJOIN020  
SJOIN021  
SJOIN022  
SJOIN023  
SJOIN024  
SJOIN025  
SJOIN026  
SJOIN027  
SJOIN028  
SJOIN029  
SJOIN030  
SJOIN031  
SJOIN032  
SJOIN033  
SJOIN034  
SJOIN035  
SJOIN036  
SJOIN037  
SJOIN038  
SJOIN039  
SJOIN040  
SJOIN041  
SJOIN042  
SJOIN043

```

DO 28 J = 1,JJ
  I1 = -2
  J1 = 7
  K1 = -3
  JM = 1
  JN = J + 1
9  I1 = I1 + 3
  I2 = I1 + 1
  I3 = I1 + 2
  J1 = J1 + 2
  J2 = J1 + 1
  K1 = K1 + 4
  K2 = K1 + 1
  K3 = K1 + 2
  K4 = K1 + 3
  SX = 0.00
  SY = 0.00
  SXX = 0.00
  SYV = 0.00
  SXY = 0.00
DO 10 I = JM,JN
  XI = X(I)
  YI = Y(I)
  SX = SX + XI
  SY = SY + YI
  SXX = SXX + XI * XI
  SYV = SYV + YI * YI
  SXY = SXY + XI * YI
10 G = JN - JM + 1
  NUM = G * SXY - SX * SY
  NUMBER = SXX * SY - SX * SXY
  DENOM = G * SXX - SX * SX
  DENO = G * SYV - SY * SY
  BETA(I1,J) = NUMBER / DENOM
  BETA(I2,J) = NUM / DENOM
  IF (G.EQ.2.00) GO TO 11
  A = DENOM * DENO - NUM * NUM

```



```

      B = A / ((G-2.00) * DENOM * DENOM)
      BETA(I3,J) = A / (G * DENOM)
      GO TO 12
11  BETA(I3,J) = 0.00
12  BETA(J1,J) = SX
      BETA(J2,J) = SXX
      IF (BETA(I3,J).GT.0.00) GO TO 13
      STD(K1,J) = 0.00
      STD(K2,J) = 0.00
      GO TO 14
13  STD(K1,J) = DSQRT((B/(G*G))*(DENOM+SX*SX))
      STD(K2,J) = DSQRT(B)
14  IF ((DENOM.LE.0.00).OR.(DENOM.LE.0.00)) GO TO 15
      STD(K3,J) = NUM/(DSQRT(DENOM)*DSQRT(DENOM))
      GO TO 16
15  STD(K3,J) = 0.102
16  IF (DABS(BETA(I2,J)).LT.1.0-50) GO TO 17
      STD(K4,J) = 1.00/BETA(I2,J)
      GO TO 18
17  STD(K4,J) = 1.070
18  IF (J.LT.(JJ - 1)) GO TO 23
      IF (J.EQ.JJ) GO TO 20
      BETA(5,J)=(BETA(1,J)+BETA(2,J)*X(N-1)-Y(N))/(X(N-1)-X(N))
      BETA(4,J) = Y(N) - BETA(5,J)*X(N)
      BETA(6,J) = 0.00
      BETA(8,J) = BETA(3,J)
      BETA(11,J) = X(N)
      BETA(12,J) = X(N) * X(N)
      DO 19 I = 5,7
19  STD(I,J) = 0.00
      STD(8,J) = 1.00 / BETA(5,J)
      JM = N
      GO TO 25
20  DO 21 I = 4,7
21  BETA(I,J) = 0.00
      BETA(8,J) = BETA(3,J)
      BETA(11,J) = 0.00

```

SJOIN044  
 SJOIN045  
 SJOIN046  
 SJOIN047  
 SJOIN048  
 SJOIN049  
 SJOIN050  
 SJOIN051  
 SJOIN052  
 SJOIN053  
 SJOIN054  
 SJOIN055  
 SJOIN056  
 SJOIN057  
 SJOIN058  
 SJOIN059  
 SJOIN060  
 SJOIN061  
 SJOIN062  
 SJOIN063  
 SJOIN064  
 SJOIN065  
 SJOIN066  
 SJOIN067  
 SJOIN068  
 SJOIN069  
 SJOIN070  
 SJOIN071  
 SJOIN072  
 SJOIN073  
 SJOIN074  
 SJOIN075  
 SJOIN076  
 SJOIN077  
 SJOIN078  
 SJOIN079  
 SJOIN080

```

      BETA(12,J) = 0.00
      DO 22 I = 5,8
      22 STD(I,J) = 0.00
      GO TO 28
      23 IF (I1.NE.1) GO TO 24
      JM = JN + 1
      JN = N
      GO TO 9
      24 BETA(8,J) = BETA(3,J) + BETA(6,J)
      25 IF ((BETA(2,J) - BETA(5,J)).GT.0.00) GO TO 26
      BETA(7,J) = 1.070
      GO TO 27
      26 BETA(7,J) = (BETA(4,J)-BETA(1,J))/((BETA(2,J)-BETA(5,J))
      27 IF(((BETA(7,J).LT.X(JM-1)).OR.(BETA(7,J).GT.X(JM))).AND.
      X (J.LT.(JJ-1))) BETA(8,J) = 1.070
      28 CONTINUE
      RETURN
      END

```

```

SJOIN081
SJOIN082
SJOIN083
SJOIN084
SJOIN085
SJOIN086
SJOIN087
SJOIN088
SJOIN089
SJOIN090
SJOIN091
SJOINQ92
SJOINC93
SJOINC94
SJOINC95
SJOINC96
SJOINC97
SJOINC98

```

```

SUBROUTINE CJOIN (N,LOCK,X,INDEX,TMIN,ITMIN,SMIN,ISMIN)      CJOIN001
*****
SUBROUTINE CJOIN CALCULATES A SERIES OF COMBINATIONS OF BEST FIT
ESTIMATES OF Y UPON X, WHICH ARE BASED ON A SIMPLE LINEAR MODEL
      Y = A1 + B1 X FOR X(1) < X < X(I)
      Y = A2 + B2 X FOR X(I) < X < X(N)
THE INDEPENDENT VECTOR X HAS LENGTH N. SEVERAL TESTS ARE APPLIED TO
MINIMIZE THE NUMBER OF MODELS ON WHICH THE CALCULATIONS MUST BE MADE.
EACH ELEMENT OF VECTOR INDEX (LENGTH = N - 2) IS KEYED TO INDICATE
WHETHER ANY TEST HAS SUCCESSFULLY ELIMINATED THE CALCULATION OF THAT
MODEL, AND IF SO, WHICH TEST. IF LOCK = 1, ALL TESTS ARE LOCKED OUT, AND
THE RSS FOR ALL MODELS IS CALCULATED. THE MINIMUM RSS FROM SJOIN (TMIN)
AND ITS INDEX (ITMIN) AND THE RSS FROM CJOIN (SMIN) AND ITS INDEX (ISMIN)
ARE FOUND. GAMMA MUST BE DIMENSIONED 5 X (N - 2).
*****
THE OUTPUT DATA ARE STORED AS:
      GAMMA(1,I) = A1, GAMMA(2,I) = B1
      GAMMA(3,I) = A2, GAMMA(4,I) = B2
      GAMMA(5,I) = COMBINED RESIDUAL SUM OF SQUARES
*****
IMPLICIT REAL*8 (A-H,O-Z)
REAL X(1)
INTEGER INDEX(1)
COMMON BETA(12,23),STD(8,23),GAMMA(5,22)
NN = N - 3
NNN = N - 2
IJK = -1
SMIN = 1.070
TMIN = 1.070
DO 4 J = 1,NNN
  DO 4 I = 1,5
    4 GAMMA(I,J) = 0.00
    INDEX(1) = 1
*****
CJOIN002
CJOIN003
CJOIN004
CJOIN005
CJOIN006
CJOIN007
CJOIN008
CJOIN009
CJOIN010
CJOIN011
CJOIN012
CJOIN013
CJOIN014

```

```

DO 5 I = 2,NNN
INDEX(I) = I
IF (LOCK.EQ.1) GO TO 5
BY TEST 1
IF (BETA(8,I-1).GE.1.D70) GO TO 5
INDEX(I) = 101
INDEX(I - 1) = 100
5 CONTINUE
6 DO 7 I = 1,NN
IF (BETA(8,I).GE.TMIN) GO TO 7
TMIN = BETA(8,I)
ITMIN = I
7 CONTINUE
IF (TMIN.EQ.1.D70) ITMIN = N/2
IF (LOCK.EQ.1) GO TO 20
BY TEST 2
DO 9 I = 2,NN
IF ((BETA(3,I-1)+BETA(6,I-1)).LT.TMIN) GO TO 9
INDEX(I) = 201
INDEX(I - 1) = 200
9 CONTINUE
C
10 J = ITMIN
GO TO 13
20 IJK = 0
11 J = 1
GO TO 13
12 J = J + 1
13 IF (J.GE.NNN) GO TO 48
IF ((INDEX(J).EQ.0).OR.(INDEX(J).GE.100)) GO TO 16
C
C
C
SELECTION OF POINT - TRY X(J+1)
INDEX(J) = 0
E = J + 1
F = N - J - 1
XX = X(J+1)
CJOIN015
CJOIN016
CJOIN017
CJOIN018
CJOIN019
CJOIN020
CJOIN021
CJOIN022
CJOIN023
CJOIN024
CJOIN025
CJOIN026
CJOIN027
CJOIN028
CJOIN029
CJOIN030
CJOIN031
CJOIN032
CJOIN033
CJOIN034
CJOIN035
CJOIN036
CJOIN037
CJOIN038
CJOIN039
CJOIN040
CJOIN041
CJOIN042
CJOIN043
CJOIN044
CJOIN045
CJOIN046
CJOIN047
CJOIN048
CJOIN049
CJOIN050
CJOIN051

```

```

D1 = E * BETA(10,J) - BETA(9,J)**2
D2 = F * BETA(12,J) - BETA(11,J)**2
G = BETA(1,J) - BETA(4,J) + XX*(BETA(2,J)-BETA(5,J))
H = (BETA(10,J)-2.D0*XX*BETA(9,J)+XX**2*E)/D1 + (BETA(12,J)-2.D0*
X XX*BETA(11,J)+XX**2*F)/D2
Z = G / H
GAMMA(1,J) = BETA(1,J) - G/(H*D1) * (BETA(10,J) - XX*BETA(9,J))
GAMMA(2,J) = BETA(2,J) + G/(H*D1) * (BETA(9,J) - XX*E)
GAMMA(3,J) = BETA(4,J) + G/(H*D2) * (BETA(12,J) - XX*BETA(11,J))
GAMMA(4,J) = BETA(5,J) - G/(H*D2) * (BETA(11,J) - XX*F)
GAMMA(5,J) = BETA(3,J) + BETA(6,J) + G**2/H
IF (GAMMA(5,J).GE.SMIN) GO TO 17
SMIN = GAMMA(5,J)
ISMIN = J
17 IF (LOCK.EQ.1) GO TO 16
C BY TEST 3
DO 14 I = 2,NNN
IF ((BETA(3,I-1)+BETA(6,I-1)).LT.SMIN) GO TO 14
INDEX(I) = 301
INDEX(I-1) = 300
14 CONTINUE
IF (BETA(8,J).EQ.1.D70) GO TO 16
X1 = BETA(9,J)/E
X2 = BETA(11,J)/F
C BY TEST 4
IF ((BETA(7,J).LT.X1).OR.(BETA(7,J).GT.X2)) GO TO 16
DO 15 I = 1,NNN
IF ((X(I + 1).GT.X2).OR.(X(I + 1).LT.X1)) GO TO 15
INDEX(I) = 400
15 CONTINUE
16 IJK = IJK + 1
IF (IJK) 11,11,12
48 SMIN = 1.D70
DO 49 I = 1,NN
IF (INDEX(I).NE.0) GO TO 49
IF (GAMMA(5,I).GT.SMIN) GO TO 49
SMIN = GAMMA(5,I)
CJOIN052
CJOIN053
CJOIN054
CJOIN055
CJOIN056
CJOIN057
CJOIN058
CJOIN059
CJOIN060
CJOIN061
CJOIN062
CJOIN063
CJOIN064
CJOIN065
CJOIN066
CJOIN067
CJOIN068
CJOIN069
CJOIN070
CJOIN071
CJOIN072
CJOIN073
CJOIN074
CJOIN075
CJOIN076
CJOIN077
CJOIN078
CJOIN079
CJOIN080
CJOIN081
CJOIN082
CJOIN083
CJOIN084
CJOIN085
CJOIN086
CJOIN087
CJOIN088

```

```

ISMIN = I
49 CONTINUE
  IF (TMIN.EQ.1.D70) ITMIN = NN
  IF (BETA(8,NNN).GE.TMIN) GO TO 52
  IF (INDEX(NNN).GE.100) GO TO 53
50 GAMMA(1,NNN) = BETA(1,NNN)
  GAMMA(2,NNN) = BETA(2,NNN)
  GAMMA(3,NNN) = BETA(4,NNN)
  GAMMA(4,NNN) = BETA(5,NNN)
  GAMMA(5,NNN) = BETA(8,NNN)
  INDEX(NNN) = 0
  IF (GAMMA(5,NNN).GT.SMIN) GO TO 51
  SMIN = GAMMA(5,NNN)
  ISMIN = NNN
51 RETURN
  C BY TEST 5
52 INDEX(NNN) = 500
53 IF (SMIN.EQ.1.D70) ISMIN = NNN
  RETURN
  END

```

```

CJOIN089
CJOIN090
CJOIN091
CJOIN092
CJOIN093
CJOIN094
CJOIN095
CJOIN096
CJOIN097
CJOIN098
CJOIN099
CJOIN100
CJOIN101
CJOIN102
CJOIN103
CJOIN104
CJOIN105
CJOIN106
CJOIN107
CJOIN108

```



```

5 FORMAT (' ',2I2,1X,8D15.5,1X,2I2)
4 CONTINUE
WRITE (NPRINT,103)
103 FORMAT ('O',11X,'STD(A1)',8X,'STD(B1)',9X,'CORR',9X,'VELO(B1)',8X,
X 'STD(A2)',8X,'STD(B2)',9X,'CORR',9X,'VELO(B2)')
DO 7 J = 1,K
N1 = J + 1 + ISHIFT
N2 = J + 2 + ISHIFT
IF (J.GE.(K-1)) N2 = 0
IF (BETA(8,J).EQ.1.070) GO TO 7
WRITE (NPRINT,5) N1,N2,(STD(I,J),I = 1,8),N1,N2
7 CONTINUE
WRITE (NPRINT,104)
104 FORMAT ('O',13X,'A1',13X,'B1',13X,'A2',13X,'B2',13X,'S')
KK = L - 2
DO 12 J = 1,KK
N3 = J + 1 + ISHIFT
IF (GAMMA(5,J).EQ.0.00) GO TO 12
WRITE (NPRINT,13) N3,(GAMMA(I,J),I = 1,5),N3,INDEX(J)
13 FORMAT (' ',2X,I2,1X,5D15.5,1X,I2,I10)
12 CONTINUE
RETURN
END

```

OUT028  
 OUT029  
 OUT030  
 OUT031  
 OUT032  
 OUT033  
 OUT034  
 OUT035  
 OUT036  
 OUT037  
 OUT038  
 OUT039  
 OUT040  
 OUT041  
 OUT042  
 OUT043  
 OUT044  
 OUT045  
 OUT046  
 OUT047  
 OUT048  
 OUT049  
 OUT050





```

1  FORMAT (' LAYER ',I2,' HAS FEWER THAN 3 DATA POINTS.')
   JJ = 1
2  A = DELTA(1,M + 1)
   B = DELTA(3,M + 1)
3  J = J + 1
   IF ((DELTA(3,M)**2 - B**2).LE.0.00) GO TO 6
   R = DSQRT(DELTA(3,M)**2 - B**2)
   IF (M.GE.2) GO TO 4
   ZETA(J,1) = A/(2.00*R)
   GO TO 6
4  T = 0.00
   DO 5 I = 1,MM
   IF ((DELTA(3,I)**2 - B**2).LE.0.00) GO TO 6
   P = DSQRT(DELTA(3,I)**2 - B**2)
5  T = T + P * ZETA(1,I)
   ZETA(J,M) = (A/2.00-T)/R
6  IF (J - 2) 10,20,30
10 A = DELTA(1,M + 1) + S(JJ) * DELTA(2,M + 1)
   B = DELTA(3,M + 1) + S(JJ) * DELTA(4,M + 1)
   D = D + ZETA(1,M)
   ZETA(4,M) = D
   GO TO 3
20 A = DELTA(1,M + 1) - S(JJ) * DELTA(2,M + 1)
   B = DELTA(3,M + 1) - S(JJ) * DELTA(4,M + 1)
   ZETA(5,M) = D - ZETA(1,M) + ZETA(2,M)
   GO TO 3
30 ZETA(6,M) = D - ZETA(1,M) + ZETA(3,M)
   RETURN
   END

```

ABYSS019  
 ABYSS020  
 ABYSS021  
 ABYSS022  
 ABYSS023  
 ABYSS024  
 ABYSS025  
 ABYSS026  
 ABYSS027  
 ABYSS028  
 ABYSS029  
 ABYSS030  
 ABYSS031  
 ABYSS032  
 ABYSS033  
 ABYSS034  
 ABYSS035  
 ABYSS036  
 ABYSS037  
 ABYSS038  
 ABYSS039  
 ABYSS040  
 ABYSS041  
 ABYSS042  
 ABYSS043  
 ABYSS044  
 ABYSS045  
 ABYSS046  
 ABYSS047

**APPENDIX B. TABULATION OF PREFERRED REGRESSION FITS**

Table 6. Tabulation of preferred regression fits

Shot no.	Location	Shot elev. m	1st vel. m/sec	2nd vel. m/sec	Depth m	Depth <sup>-</sup> m	Depth <sup>+</sup> m	3rd vel. m/sec	Depth m	Depth <sup>-</sup> m	Depth <sup>+</sup> m
07	1-04E	357.3	3365(18) <sup>a</sup>								
08	1-04E	356.6	3131(09)	4189(14)	61.7	81.5	44.7				
10	1-03E E <sup>b</sup>	354.2	1859(05)	2212(07)	30.5	37.5	24.3	3761(11)	120.2	189.7	68.4
09	1-03E E	354.8	1887(06)	2268(07)	35.7	70.2	13.8	4263(07)	138.3	255.7	61.5
11	1-03E W	356.8	1886(04)	2810(21)	30.4	41.7	20.0				
12	1-02E	363.0	1805(11)	2534(12)	74.7	81.9	67.9				
13	1-02E	359.1	1890(12)	2526(11)	81.3	112.3	55.7				
02	1-01E	359.6	1871(08)	2253(09)	41.7	103.9	8.1	3657(08)	159.4	211.1	117.8
01	1-01W	364.5	1796(08)	4423(15)	77.2	86.5	68.2				
02	1-01W	363.5	1679(02)	3292(22)	22.6	26.1	19.2				
01	2-04E	358.9	1817(09)	4699(15)	98.6	111.9	85.9				
01	2-04E	358.9	2339(06)	3433(19)	45.9	76.1	21.0				
04	2-03E	368.4	2202(05)	3515(16)	46.4	57.8	35.7				
03	2-03E	368.2	1735(04)	3140(19)	32.9	36.3	29.5				
06	2-02E	361.2	1823(03)	2909(07)	26.7	43.4	13.2	3218(12)	61.9	96.3	38.4
05	2-02E	360.7	1883(04)	3117(14)	30.9	40.9	21.6				
04	2-01E	361.1	2576(06)	3159(13)	36.5	58.8	18.2				
03	2-01E	358.9	1752(08)	3850(16)	68.1	78.7	58.1				
03	2-01W	364.2	1881(12)	2655(12)	81.2	107.3	59.0				
04	2-01W	362.5	1890(11)	2562(13)	73.2	93.6	55.4				
01	2-02W	361.5	1809(08)	2730(14)	80.1	91.2	69.7				
02	2-02W	361.1	1843(09)	2080(06)	35.8	74.5	12.5	2800(08)	114.8	179.4	68.7
04	2-03W	370.3	1927(11)	3103(13)	90.2	101.3	79.8				
03	2-03W	370.3	1898(14)	2960(10)	95.1	148.5	54.5				
02	3-05E	354.7	4370(04)								
01	3-05E	356.2	3000(02)	4839(04)	25.4	- <sup>c</sup>	-				
02	3-04E	361.2	1855(04)	2164(07)	22.9	39.0	11.1	3087(12)	91.1	113.6	71.4
01	3-04E	361.0	1886(09)	3132(14)	78.1	85.9	70.7				
03	3-03E	360.8	1878(14)	3058(08)	105.2	120.9	90.7				
04	3-03E	363.1	1867(11)	2939(11)	99.0	113.1	86.0				

07	3-02E	369.2	1867(08)	2423(09)	58.2	83.2	38.3	3877(05)	169.0	307.7	86.3
08	3-02E	364.9	1823(07)	2322(08)	44.2	63.2	28.8	3108(09)	124.4	162.3	93.8
06	3-01E	367.5	1838(10)	2205(05)	52.5	-	-	3525(09)	152.9	177.4	131.1
05	3-01E	364.7	1849(09)	2428(07)	64.5	99.6	37.9	3442(09)	160.6	238.6	104.8
08	3-01W	363.4	1707(02)	1916(11)	10.1	20.1	2.4	2457(12)	74.9	89.8	61.4
07	3-01W	368.8	1829(03)	2259(09)	46.0	58.9	34.9	2467(12)	92.5	168.6	49.0
06	3-02W	369.5	1792(06)	2218(17)	35.9	44.4	28.1				
05	3-02W	369.0	1905(08)	2238(04)	58.1	171.4	11.9	2544(10)	105.2	153.5	71.2
06	3-03W	377.1	1847(12)	2845(10)	95.8	122.6	72.6				
05	3-03W	378.5	1853(07)	2133(02)	41.9	-	-	2934(15)	95.6	115.1	78.4
02	4-06E	358.9	1781(02)	4776(10)	16.5	20.3	12.8				
02	4-06E	358.9	4619(11)								
02	4-05E	358.1	1747(07)	2309(15)	45.4	56.3	35.5				
01	4-05E	355.2	1638(06)	2326(18)	40.1	68.3	17.1				
03	4-04E	362.2	1845(07)	2252(13)	46.0	57.7	35.5	3203(04)	166.6	169.4	163.9
04	4-04E	359.0	1828(09)	2373(10)	55.2	72.1	40.5	2642(05)	116.2	-	-
06	4-03E	366.6	1864(08)	2290(06)	47.8	75.7	27.6	3931(10)	148.3	169.0	129.5
05	4-03E	367.1	1855(05)	2355(05)	37.5	70.7	16.3	2847(12)	77.6	118.2	48.5
07	4-02E	368.7	1903(06)	2113(12)	32.5	69.3	9.5	3797(06)	184.1	260.2	125.5
08	4-02E	370.9	1915(14)	2831(08)	111.1	162.8	70.9				
02	4-01E	367.0	1825(10)	3977(14)	102.5	110.4	94.7				
01	4-01E	368.4	1897(10)	4019(14)	108.5	122.4	95.3				
04	4-01W	372.7	1820(10)	2350(13)	64.0	74.1	54.7				
03	4-01W	370.3	2032(02)	2315(18)	45.9	90.7	15.7				
07	4-02W	376.8	1862(11)	2226(11)	54.4	80.1	34.0				
08	4-02W	375.2	1812(09)	2225(14)	50.6	57.0	44.7				
01	4-03W	372.9	1815(10)	2279(13)	67.2	92.3	46.1				

<sup>a</sup>Number of points on line segment.

<sup>b</sup>Where not indicated, the shot with cable strung east or north is listed first at each station.

<sup>c</sup>Indicates wide statistical limits.

Table 6. (Continued)

Shot no.	Location	Shot elev. m	1st vel. m/sec	2nd vel. m/sec	Depth m	Depth <sup>-</sup> m	Depth <sup>+</sup> m	3rd vel. m/sec	Depth m	Depth <sup>-</sup> m	Depth <sup>+</sup> m
02	4-03W	375.6	1775(10)	2228(11)	59.1	75.8	44.4				
05	4-04W N	378.6	1836(13)	4840(10)	137.7	153.1	123.2				
03	4-04W S	379.1	1997(07)	3596(05)	100.2	120.5	82.2				
04	4-04W N	378.5	1837(12)	4371(07)	128.4	168.0	94.8				
01	5-06E	352.3	3756(08)	5701(05)	60.2	-	-				
01	5-06E	352.3	3682(04)	4747(08)	32.3	47.7	19.9				
01	5-05E	367.1	1839(06)	2020(17)	19.1	64.0	-				
02	5-05E	363.8	1861(12)	2251(11)	63.4	97.3	37.3				
03	5-04E	350.9	1893(11)	2468(13)	62.8	78.4	49.0				
04	5-04E	357.1	1765(11)	2672(13)	82.8	91.5	74.5				
06	5-03E	359.7	1820(08)	2296(16)	48.7	56.1	41.7				
05	5-03E	361.2	1829(09)	2133(02)	50.2	-	-	2586(13)	102.9	129.5	80.9
07	5-02E	369.7	1801(06)	2130(16)	42.8	58.8	29.3	2909(02)	172.9	-	-
08	5-02E	369.6	1742(04)	1926(13)	15.6	23.9	8.6	2545(07)	115.4	158.1	88.6
09	5-01E	371.9	1816(11)	3484(12)	81.8	89.3	74.7				
10	5-01E	374.3	1852(09)	3587(15)	88.7	97.1	80.6				
02	5-01W	371.2	1748(04)	4790(07)	43.2	50.5	36.3				
04	5-01W	372.1	1683(03)	3788(15)	27.1	31.7	22.6				
02	5-02W	368.1	1757(07)	2148(12)	43.3	80.1	18.2	7442(04)	248.3	302.9	201.3
01	5-02W	373.0	1770(12)	2290(10)	62.1	106.8	30.3				
04	5-03W	371.9	1797(11)	2279(13)	61.7	75.8	49.0				
03	5-03W	368.5	1780(11)	2254(12)	63.0	94.4	38.0				
05	5-04W	376.2	1820(11)	2260(10)	62.2	88.2	41.0				
06	5-04W	377.6	1486(05)	2190(17)	35.5	45.7	26.0				
07	5-05W	379.0	1793(11)	2344(11)	68.5	95.1	46.8				
08	5-05W	377.1	1826(11)	2342(07)	68.5	110.1	37.7				
06	5-06W	381.6	1887(15)	6379(09)	185.6	220.7	153.9				
05	5-06W	379.5	1730(04)	3219(16)	60.3	74.7	46.7				
04	6-16E E	342.6	1756(02)	3207(06)	12.1	36.9	-	4462(05)	49.7	83.4	26.8
04	6-16E N	342.6	1870(02)	3012(06)	10.8	23.6	1.1	4562(05)	52.9	-	-

03	6-15E E	347.4	2770(04)	3800(03)	25.4	-	-	6006(05)	64.0	82.1	49.1
03	6-15E S	347.4	1626(02)	4574(09)	17.1	20.6	13.7				
01	6-14E	347.5	1679(02)	3077(05)	23.4	59.0	1.0	6275(05)	87.2	178.3	34.4
01	6-14E	347.5	1595(02)	4764(09)	23.1	39.6	24.9				
02	6-13E N	349.0	1761(02)	3982(10)	25.2	33.6	17.3	5360(09)	100.6	187.8	46.3
01	6-13E N	359.4	2061(03)	5417(06)	49.3	55.2	43.7				
01	6-13E S	359.4	1762(04)	4540(07)	37.8	51.4	25.6				
01	6-12E	347.0	1791(05)	5271(07)	51.6	62.1	41.9				
01	6-12E	347.0	2253(08)								
01	6-11E E	351.1	1736(05)	2115(06)	27.4	60.9	7.1				
01	6-11E W	351.1	1727(03)	1912(08)	13.7	25.0	5.4				
02	6-11E W	351.7	1682(02)	2058(08)	21.4	33.4	11.5	2357(12)	66.9	141.0	24.8
01	6-10E	349.0	1781(04)	2384(07)	27.3	48.2	11.5				
01	6-10E	349.0	2127(02)	2347(08)	13.7	35.2	1.3				
01	6-09E	355.8	1799(07)	2000(04)	31.3	-	-				
01	6-09E	355.8	1869(07)	2406(04)	50.1	101.2	20.6				
02	6-08E	342.5	1752(07)	2269(04)	43.7	-	-	2909(02)	89.5	-	-
02	6-08E	342.5	1860(04)	2133(05)	30.1	71.8	8.5				
03	6-07E	359.3	1846(11)								
03	6-07E	359.3	1684(05)								
01	6-06E E	366.4	1822(08)	2000(03)	33.7	33.8	33.7				
01	6-06E W	366.4	1813(07)	2148(04)	42.3	-	-				
02	6-06E E	365.5	1843(11)	2346(11)	60.4	68.2	53.2				
03	6-05E E	361.0	1842(08)	2043(04)	34.4	-	-				
03	6-05E W	361.0	1858(05)	2717(04)	33.7	-	-				
04	6-05E E	365.9	1894(08)	2384(11)	67.2	83.7	52.7				
05	6-04E E	365.1	1514(02)	1907(09)	12.6	17.1	8.0				
05	6-04E W	365.1	1831(06)	2034(05)	31.3	-	-				
06	6-04E E	366.9	1854(11)	2284(11)	56.2	73.8	41.0				
07	6-03E E	372.1	1752(07)	2158(04)	35.4	-	-				
07	6-03E W	372.1	1852(07)	2015(05)	28.9	-	-				
08	6-03E E	373.0	1764(06)	1957(07)	26.5	49.3	11.1	3377(07)	141.5	214.4	87.6
03	6-02E E	374.0	1744(06)	3247(05)	49.5	107.0	12.5				
03	6-02E W	374.0	1727(03)	4258(06)	47.9	63.7	33.9				
04	6-02E E	374.6	1745(04)	3811(18)	36.0	69.6	6.9				
06	6-01E	371.8	2059(03)	3889(18)	33.3	45.9	21.6				
05	6-01E	370.0	1826(03)	3464(07)	32.9	36.1	29.8	4380(10)	89.2	121.5	63.4
06	6-01W W	373.3	1806(03)	3961(17)	35.3	39.6	31.0	8000(02)	236.4	-	-

Table 6. (Continued)

Shot no.	Location	Shot elev. m	1st vel. m/sec	2nd vel. m/sec	Depth m	Depth <sup>-</sup> m	Depth <sup>+</sup> m	3rd vel. m/sec	Depth m	Depth <sup>-</sup> m	Depth <sup>+</sup> m
05	6-01W E	373.3	1317(03)	4066(08)	31.6	36.6	26.7				
05	6-01W W	373.3	1455(02)	4103(09)	36.1	44.2	28.4				
07	6-02W E	368.2	1697(03)	3682(07)	31.2	39.1	23.8				
07	6-02W W	368.2	1772(02)	4507(04)	34.9	51.3	21.5				
08	6-02W W	373.3	1585(02)	3467(09)	26.5	31.4	21.8	4788(09)	89.5	161.1	44.0
04	6-03W	371.7	1831(07)	3979(13)	80.9	89.6	72.5				
03	6-03W	372.5	1888(04)	3069(07)	36.8	50.1	25.5	3414(12)	71.2	131.3	36.6
01	6-04W	374.6	1853(08)	2601(08)	55.1	132.8	12.0	4007(06)	160.3	231.5	107.7
02	6-04W	372.7	1815(07)	3779(14)	72.6	90.8	56.0				
05	6-05W E	375.7	1842(11)								
05	6-05W W	375.7	1844(11)								
06	6-05W E	373.9	1919(14)	3812(05)	143.9	162.5	126.7				
01	6-06W E	372.4	1672(05)	4814(07)	50.9	59.2	42.9				
01	6-06W W	372.4	1957(04)	3829(06)	46.5	54.7	38.8				
02	6-06W E	372.4	1735(04)	4388(07)	53.2	70.1	37.8				
03	6-07W	369.1	1780(05)	3794(06)	60.3	75.6	46.8				
03	6-07W	369.1	1822(07)	3368(05)	69.6	82.7	57.9				
04	6-07W W	369.8	1764(05)	3214(10)	45.2	61.8	30.3				
01	6-08W	369.2	1856(10)								
01	6-08W	369.2	1870(10)								
02	6-08W	373.8	1835(09)	2611(11)	86.3	131.2	51.4				
08	6-09W	375.5	1785(10)	2279(14)	63.8	90.0	42.1				
07	6-09W	375.5	1857(13)	2623(10)	95.9	118.5	75.5				
03	7-07E	346.6	1724(03)	4295(09)	34.5	40.5	28.8				
03	7-07E	346.6	3746(06)	6809(05)	80.7	-	-				
04	7-06E	349.5	1707(05)	4647(06)	55.5	71.2	41.6				
04	7-06E	349.5	1775(03)	4167(08)	45.4	53.2	38.0				
05	7-05E	350.8	1728(04)	1920(08)	21.1	50.1	4.6				
05	7-05E	350.8	1793(07)	2777(05)	41.0	-	-				
02	7-04E	352.6	1779(10)	2441(14)	70.6	89.0	54.4				



01	7-04E	349.8	1717(11)	2396(12)	67.4	90.4	47.8			
04	7-03E	355.4	1838(10)	2686(14)	75.5	85.5	66.0			
03	7-03E	356.5	1835(12)	2692(12)	77.2	95.9	60.7			
06	7-02E	362.7	1794(10)	2321(13)	64.6	80.7	50.3			
05	7-02E	364.4	1628(10)	2343(14)	60.6	68.1	53.4			
08	7-01E	371.6	1858(11)	2237(13)	58.3	72.5	45.8			
07	7-01E	369.3	1925(10)	2271(14)	61.3	78.5	46.4			
06	7-01W	372.4	1826(05)	2134(08)	25.2	56.8	6.4	3693(12)	113.0	130.9
05	7-01W	375.9	1825(09)	3212(11)	87.9	101.8	75.0			96.9
04	7-02W	375.4	1806(09)	3194(10)	75.9	113.2	45.5			
03	7-02W	375.8	1808(09)	3575(11)	90.1	114.0	68.8			
01	7-03W	367.2	1781(06)	3455(14)	60.2	75.2	46.5			
02	7-03W	369.5	1786(06)	2858(06)	60.6	119.5	22.2			
01	7-04W	370.9	1760(10)	2315(12)	59.4	69.9	40.8			
02	7-04W	365.4	1780(09)	2376(11)	67.2	84.2	54.1			
03	7-05W	375.8	1813(06)	2192(04)	38.4	-	-			
03	7-05W	375.8	1762(04)	1955(07)	26.2	40.2	15.4			
04	7-06W	375.1	1801(07)	2667(02)	81.5	-	-			
04	7-06W	375.1	1662(05)	1998(06)	27.5	37.7	18.9			
01	8-06E	348.2	1868(07)	5335(16)	75.8	79.4	72.3			
02	8-06E	346.8	1800(07)	5338(18)	74.6	77.4	71.7			
03	8-05E E	352.1	1816(07)	2251(06)	45.1	-	-	5333(09)	165.4	177.6
02	8-04E	355.0	1839(12)	2366(11)	69.1	112.3	36.9			153.8
01	8-04E	348.3	1653(06)	2287(12)	49.1	61.7	37.8			
06	8-03E	364.2	1855(13)	2736(10)	92.2	126.3	63.9			
05	8-03E	364.8	1910(15)	3213(07)	131.5	242.7	58.4			
07	8-02E	365.7	1828(12)	2188(11)	54.5	103.5	20.9			
08	8-02E	365.4	1898(14)	2471(08)	86.2	112.5	64.0			
03	8-01E	367.3	1826(10)	2588(12)	70.1	78.2	62.5			
04	8-01E	367.7	1872(12)	2902(10)	94.5	110.6	79.7			
02	8-01W	369.1	1869(15)	2372(07)	83.1	161.2	33.9			
01	8-01W	372.7	1926(15)	2314(07)	78.0	150.2	32.9			
05	8-02W	372.7	1788(09)	2299(08)	56.1	68.1	45.4	3544(06)	164.6	208.9
06	8-02W	370.1	1746(07)	2090(08)	35.7	66.6	15.1	3038(09)	122.2	157.9
03	8-03W	368.7	1822(12)	3617(09)	102.2	116.1	89.1			128.2
04	8-03W	370.1	1739(08)	3088(13)	64.9	68.9	61.0			92.5
02	8-05W	373.0	1866(14)	2701(09)	100.7	125.6	78.9			

Table 6. (Continued)

Shot no.	Location	Shot elev. m	1st vel. m/sec	2nd vel. m/sec	Depth m	Depth <sup>-</sup> m	Depth <sup>+</sup> m	3rd vel. m/sec	Depth m	Depth <sup>-</sup> m	Depth <sup>+</sup> m
01	8-05W	371.9	1874(16)	3324(07)	143.6	181.0	111.4				
01	9-05E	359.2	1881(07)	3200(02)	66.6	-	-				
02	9-05E	358.5	1825(07)	2942(02)	59.1	-	-	5017(12)	124.4	148.8	103.3
01	9-04E	354.0	1918(10)	2607(08)	74.4	111.9	45.3	5086(12)	125.1	147.6	105.0
02	9-04E	357.9	1933(10)	2771(09)	90.2	114.6	69.2				
04	9-03E	356.2	1914(08)	2403(10)	75.3	91.3	61.0				
03	9-03E	361.3	1979(15)	2538(07)	102.5	249.9	28.7				
05	9-02E	360.2	1646(09)	3051(13)	91.7	120.9	66.3				
06	9-02E	357.8	1783(07)	2876(16)	59.2	73.1	46.4				
07	9-01E	367.4	2020(10)	2799(14)	77.6	83.7	71.8				
08	9-01E	364.9	1836(08)	2631(16)	60.3	67.1	53.8				
01	9-01W	373.0	1758(05)	3071(16)	41.1	49.7	32.9				
02	9-01W	376.2	1839(07)	2471(08)	52.7	67.1	40.3	5091(07)	181.4	214.2	152.6
04	9-02W	368.0	1841(10)	2831(13)	83.5	93.4	74.1				
03	9-02W	363.7	1873(11)	2886(12)	93.0	109.9	77.5				
06	9-03W	372.9	1802(08)	2716(15)	70.4	80.9	60.6				
05	9-03W	370.6	1790(11)	2807(13)	81.3	96.2	67.6				
02	10-5E	347.6	1867(07)	2667(03)	49.8	-	-				
01	10-5E	350.1	1842(09)	4005(02)	91.1	-	-				
03	10-3E	351.3	1937(13)	3404(04)	153.1	306.2	63.1				
04	10-3E	353.9	1901(08)	2422(12)	67.7	85.7	52.0				
05	10-2E	356.9	1868(09)	2903(13)	63.9	69.5	58.6				
06	10-2E	356.7	1855(08)	2901(14)	62.3	71.6	53.6				
07	10-1E	356.6	1789(05)	2973(18)	42.5	66.0	21.9				
08	10-1E	359.6	1806(05)	3167(15)	62.9	71.3	54.8				
03	10-1W	374.7	1868(10)	3462(13)	88.3	100.7	76.7				
04	10-1W	369.4	2006(09)	3470(14)	84.8	91.9	77.9				
09	10-2W	364.7	1856(11)	3281(12)	99.7	113.9	86.4				
10	10-2W	364.6	1848(08)	2795(16)	62.1	80.8	45.4				
08	10-3W	373.0	1887(16)	2377(08)	92.1	141.4	55.6				
								5035(10)	127.1	140.5	114.4
								5345(11)	141.5	170.5	117.5

07	10-3W	370.1	1879(11)	2267(08)	76.5	215.2	13.0	5312(14)	94.5	99.7	89.4
06	11-1E	357.7	1936(06)	2133(02)	14.4	-	-				
05	11-1E	356.6	2003(07)	5433(15)	89.7	95.3	84.2				
08	11-1W	367.7	1804(06)	4776(15)	68.6	73.1	64.2				
07	11-1W	367.7	1753(12)	4965(10)	73.9	75.9	72.0				